UDC 620.178.3:
539.43:
629.73.02.018.4

TECHNICAL MEMORANDUM OF NATIONAL AEROSPACE LABORATORY

TM-394T

Review of Aeronautical Fatigue Investigations in Japan 1977-1979

Tadao KAMIYAMA and Soushiro IIDA

October 1979

NATIONAL AEROSPACE LABORATORY

CHŌFU, TOKYO, JAPAN

TABLE OF CONTENTS

(* The Technical Research and Development Institute, Japan Defence Agency)

Item	Author
General	Tadao KAMIYAMA*, Soushiro IIDA** Kazuyuki TAKEUCHI*** Hiroo ASADA***
Chapter 1	Tadao KAMIYAMA*
Chapter 2	Koichi ONO***, Ippei SUSUKI** Toshio NOHARA***, Soushiro IIDA** Toshiyasu FURUTA***
Chapter 3	Shigetaka TOYOHIRA**** Shiro MIYAKE****
Chapter 4	Tadao KAMIYAMA*
Chapter 5	Makoto HIRAHARA*****
Chapter 6	Hiroshige KIKUKAWA******
Chapter 7	Tetsuo UCHIMOTO*******
Chapter 8	Kohei SAITO******** Shun-ichi BANDO******** Koji ITO********

* The Aircraft Accident Investigation Commission

** Second Airframe Division

*** First Airframe Division

**** The Third Research Center, The Technical Research and Development Institute, Japan Defence Agency

***** Civil Transport Development Corporation

****** Fuji Heavy Industries, Ltd., Aircraft Division

******* Mitsubishi Heavy Industries, Ltd., Aircraft Works

******** Kawasaki Heavy Industries, Ltd., Aircraft Group

Review of Aeronautical Fatigue Investigations in Japan 1977-1979*

Tadao KAMIYAMA** and Soushiro IIDA***

概　　要

国際航空機疲労委員会（ICAF）の第16回会議は，昭和54年5月14日と15日の2日間にわたり，ベルギー国のブラッセル市において開催された。

本報告は，この会議において，日本における最近2年間の航空機疲労に関する研究の展望として発表するために，航空宇宙技術研究所，防衛庁技術研究本部第3研究所，航空事故調査委員会，民間輸送機開発協会および各航空機製造会社で行なわれた航空機疲労の研究をまとめたものである。

1. INTRODUCTION

After the fifteenth meeting of the ICAF, the sixth sub-committee on Aeronautical Fatigue of the 129th Committee on Strength, Fracture and Fatigue of the Japan Society for Promotion of Sciences collected twenty-three papers presented by Japanese authors and distributed to ICAF member countries from National Aerospace Laboratory. The title of those ICAF Documents are listed in the references at the end of this review.

The full scale fatigue tests of Model 700/710, twin engine general usage aircraft, were terminated in April of 1978 at the Fuji Heavy Industries. The full scale vibration and drop fatigue test on helicopter type HSS-2 (Sikorsky S-61) are now underway at the Third Research Center, the Technical Research and Development Institute, Japan Defence Agency.

This paper is the review of the investigations on aeronautical fatigue problems during the last two years, conducted in National Aerospace Laboratory, the Third Research Center, Aircraft Accident Investigation Commission, Civil Transport Development Corporation, and three representative airplane manufacturers, Fuji, Mitsubishi and Kawasaki Heavy Industries.

* Received August 31, 1979

** The Aircraft Accident Investigation Commission
*** Second Airframe Division

Presented at the 16th Conference of the International Committee on Aeronautical Fatigue, held on May 14 – 15, 1979 at Brussels, Belgium.

2. NATIONAL AEROSPACE LABORATORY, THE SCIENCE AND TECHNOLOGY AGENCY

2.1 Data Collection of the Gust Loads

National Aerospace Laboratory (NAL) has been collecting gust data in domestic scheduled flgihts from the records of DFDR's (Digital Flight Data Recorders) equipped on Lockheed L-1011 transports of All Nippon Airways[1].

The results presented here were obtained from an analysis of 1,070 flights of data covering about 1,500 flight hours and 760,000 km of flight distance. The overall data contained 10,605 turbulence patches, and maximum and minimum vertical acceleration were 1.77 g and 0.21 g, respectively. The cumulative frequencies of derived gust velocities for the whole records are shown in Fig. 1. Also shown are the cumulative frequencies of derived gust velocities obtained from Douglas DC-4 domestic scheduled flights by TAKEDA in 1960, and those for clear air turbulence in the Northern Hemispere at high altitudes by Steiner[2]. Comparing the corresponding altitude bands, the results of the present analysis shows a good coincidence with those two curves.

The percentages of the flight time in the turbulence patches to the total flight time are shown in Fig. 2. Also shown are the values of P_1 (percentage of flight

time in non-storm turbulence) adopted in U. S. MIL. Spec[3]. The lengths of turbulence patches were obtained from air speed and flight time in turbulence patches, and cumulative frequencies of the patch lengths are shown in Fig. 3. The variations of mean and RMS values of the patch lengths with altitude are shown in Fig. 4. Fig. 4 shows that the lengths of turbulence patches are nearly constant excluding both very low and high altitude.

2. 2 Evaluation of Fatigue Crack Growth Rates under Random Loads

(1) Introduction

Many airframe structures are subjected to complex fluctuating load sequence. The evaluation of the fatigue crack growth rates under random loads is one of the most important problems to attain high reliability and safety of those structures. The fracture mechanics approach has become a useful engineering tool in treating the mechanics of subcritical crack growth, and has been employed in the present study of the random loading crack propagation behavior of a steel JIS-S45C and an aluminum alloy 2024-T3.

The evaluation method presented here is based on the combination of Miner's linear cumulative damage rule on crack growth and a new cycle counting method of random wave called Hysteresis-Loop Counting Method (HL method).

(2) Hysteresis-Loop Counting Method

There are various cycle counting methods, which are mainly developed to estimate the fatigue damage under complex stress or strain histories. Among them, the peak counting and the level crossing counting method are most commonly used because of their simplicity. The former counts merely the number of peaks, and the latter counts that of crossings certain levels with positive or negative slope. It is obvious both these methods do not pay any attention to the sequential order of peaks and troughs. However, it is generally accepted that the fatigue damage is closely related to the stress-strain time history, in the other words, the total energy consumption during the complex changes of loading. Therefore it is desirable to take into account the sequential order of peaks and troughs for the accurate evaluation of the fatigue damage.

From this point of view, the range pair, rain flow and full wave counging methods are more reasonable as they are intended to evaluate the closed hysteresis loops. Up to now, many experimental data have shown that these methods predict the fatigue damage more accurately than the others.

But none of them counts closed hysteresis loops perfectly in the strict sense. This error in counting is negligibly small for the high-cycle fatigue life estimation, but not so small for the low-cycle case.

The HL method, proposed here, is improved to be able to count the closed hysteresis loops correctly and simplified in algorithm. The new method is suitable for the on-line real time data processing, and powerful for numerous data treatment.

An example of application of the HL method is shown in Fig. 5. This joint distribution of the range and the mean is a counting result of a random wave whose power spectral density function (PSD) is

$$H(\omega) = \frac{{\omega_0}^2}{({\omega_0}^2 - \omega^2) + 2j\zeta\omega_0\,\omega}, \quad \zeta = 0.5$$

where the angular frequency, ω (rad/sec) is used instead of the frequency $f = \omega/2\pi$ (Hz), ω_0 denotes the natural angular frequency, ζ is damping ratio.

A set of the range and the mean is calculated by one peak and one trough which define a closed hysteresis loop.

In this study, the time history of random wave is considered as that of the stress intensity factor, K value. An equivalent value of the stress intensity factor range ΔK_{eq} which gives the prediction rate of fatigue crack growth is derived from the joint distribution of the range ΔK and the mean K_m. The joint distribution of ΔK and K_m may well be described in terms of ΔK and R, where $R = K_{min}/K_{max}$, $K_{max} = K_m + 0.5\Delta K$ and $K_{min} = K_m - 0.5\Delta K$. The probability density function of the joint distribution of ΔK and R, $p(\Delta K, R)$ will be adopted in the following discussion.

(3) Comparison of Test Results with Calculation

Fatigue crack growth under stationary random loads was observed in plates of a carbon steel JIS S45C and an aluminum alloy 2024-T3 at the stress level of small scale yielding, and the crack growth rates were compared with the predicted rates from the test data under constant amplitude loads.

The center-cracked strip specimens of rolling direction were cut from cold-rolled plate, 150 mm wide, 4mm and 6mm thick for the steel and the Al-alloy, respectively as shown in Fig. 6. The fatigue tests under the constant amplitude loads and the random loads were conducted by the electro-hydraulic servo-controlled fatigue testing machine.

The crack growth rates in constant amplitude tests da/dN and their dependency on the stress ratio $R = \sigma_{min}/\sigma_{max}$ were expressed approximately as follows, especially for the steel.

$$da/dN = C_0 \left[\alpha \cdot \Delta K \right]^m \qquad (1)$$

where ΔK is the range of the stress intensity factor $K\ [kgf \cdot mm^{-3/2}]$, C_0 is a constant, and 3.96×10^{-15} for S45C and 1.29×10^{-12} for 2024-T3, m is 3.02 and 2.39, $\alpha = 1 + 0.29\sqrt{R}$ and $1 + 0.68R$, respectively as shown in Fig. 7.

The Gaussian stationary random load waves used in the tests were generated by filtering the output of a Gaussian white noise generator through two types of linear electronic filters, the displacement-to-acceleration response of the vibration system of one degree of freedom system (1 D.F.) and the Butterworth filter of variable band width (B.F.).

The power spectral density functions (PSD) for both waves are proportional to

$$H(\omega) = \left| \frac{\omega_0^2}{(\omega_0^2 - \omega^2) + 2j\zeta\omega_0\,\omega} \right| \qquad (1D.F.)$$

$$H(\omega) = \left| \frac{1}{\prod_{i=1}^{6} (j\omega/\omega_L - a_i) \prod_{i=1}^{6} (\omega_H/j\omega - a_i)} \right| \qquad (B.F.)$$

where $j = \sqrt{-1}$, $a_i = \exp\left[(5 + 2i/12)\pi j \right]$, ω_L and ω_H are the cut-off angular frequencies of the low-pass and the high-pass filter units, respectively.

Let the relation of Eq. (1) be $da/dN = \Psi(\Delta K, R)$, and the probability density of the joint distribution be $p(\Delta K, R)$, which is obtained by the above-mentioned hysteresis loop counting method, and assume Miner's linear cumulative rule on the crack growth. And an equivalent range of stress intensity factor ΔK_{eq} can be so defined that the same growth rate as predicted one will be given under a constant amplitude test of ΔK_{eq} in case of $R = 0$, namely ΔK_{eq} is given by the relation

$$\Psi(\Delta K_{eq}, 0) = \int_0^\infty \int_0^1 \Psi(\Delta K, R) \cdot p(\Delta K, R) \cdot dR \cdot d(\Delta K) \qquad (2)$$

The effect of the unclosed loop on damage should be added as the effect of the sum of the half cycles, if necessary.

The solid lines in Fig. 8 and 9 are all the predicted growth rates. The experimental data in Fig. 8 are plotted in terms of ΔK_{eq} in the same logarithmic scale as that of ordinate but shifted horizontally by arbitrary amount to avoid confusion, and the solid line is the predicted line, namely da/dN - ΔK relation under the conditions of ΔK = constant and $R = 0$.

Agreements between experiment and prediction are excellent for the steel, not only under the random loads of narrow band but also of wide band, and not so good but satisfactory for Al 2024-T3. Some experimental data as shown in Fig. 9 lie near the predicted solid lines, but the slopes become slightly different.

2. 3 The Fatigue Crack Propagation under Flight-by-Loading

Flight simulation load tests were carried out on sheet specimens of 2024-T3 clad material. The standardized load sequence for flight simulation load tests on transport aircraft wing structures proposed by LBF and NLR, was applied. The spectrum is illustrated in Fig. 10.

The main objectives of this study were to investigate the effect of following modifications of the load sequence on crack propagation life.

(1) Truncation of infrequently occurring high amplitude gust cycles.

(2) Omission of low amplitude gust cycles.

(3) Omission of ground-to-air cycles.

An example of the load recording during a random test is shown in Fig. 11. Comparative results of crack propagation tests are presented in Fig. 12. The results are summarized as below.

(1) The truncation of infrequently occurring high amplitude gust cycels accelerated the rate of crack propagation considerably.

(2) The omission of low amplitude gust cycles in-

creased the crack propagation life.

(3) The omission of the ground-to-air cycles increased the crack propagation life.

2.4 The Effect of Load Sequence on Fatigue Crack Propagation under Program Loading and Random Loading

The sequence of fatigue test loads have a significant influence on the crack propagation. The crack propagation was studied on 2024-T3 Alclad sheet specimens under program loading and random loading with a short block period and long block period. In the program tests, Low-High, High-Low and Low-High-Low sequences were applied.

An example of the load recording during the program tests and a random test is shown in Fig. 13. Comparison of test results are presented in Figs. 14 and 15. Figs. 14 and 15 show that the crack propagation rates under program and random loading were significantly different. The results are summarized as below.

(1) In the program test, three load sequences were applied, namely Low-High-Low, Low-High and High-Low, in this order the crack propagation life was increased.

(2) The crack propagation life in random loading located about in the middle of those of three program loadings.

2.5 Acoustic Fatigue Strength of GFRP Panel

Experimental study on the acoustic fatigue strength of GFRP panels with or without CFRP stiffener was conducted at NAL, using the acoustic fatigue test facility. The panels with two kinds of CFRP stiffener, those are bonded stiffener and integrated stiffener, were tested.

Fig. 16 shows the equivalent S-N curves for panels with or without CFRP stiffener. The results show that the acoustic fatigue strength of GFRP panel with CFRP stiffener was considerably greater than those of GFRP panel without stiffener. Especially, the integrated stiffener was more effective than the bonded stiffener at the high sound pressure level, because of debonding was not caused in the integrated stiffener, while debonding was caused in the bonded stiffener.

2.6 Plane Bending Fatigue Strength of Soaked CFRP Laminated Plates

The experimental investigation on the plane bending fatigue strength of three kinds of soaked CFRP laminated plates was conducted at NAL.

The composites consist of denatured epoxy resin MRX-3501, #241, #3130 and carbon fiber, PYROFIL-XAS made by Mitsubishi Rayon Co., CARBOLON Z-3 by Nippon Carbon Co., and TORAYCA T-300 by Toray Co.

These laminated CFRP plates were fabricated with 24-ply of [0°, 45°, -45°, 90°] symmetrical laminates, and soaked in water for two weeks. The plane bending fatigue strength of soaked CFRP laminated plates was compared with those of unsoaked, normal CFRP laminated plates. The results were shown in Fig. 17 to 19 with the form of S-N curves.

It was found that there was no difference of plane bending fatigue strength between the soaked CFRP laminated plate and the unsoaked CFRP laminated plate of XAS/MRX-3501 and X-3/#241, when the composite soaked weight percentage is less than 0.24%. But the plane composite soaked weight percentage is less than 0.24%. But the plane bending fatigue strength of soaked CRFP laminated plate of T-300/#3130 was slightly lower than that of unsoaked one. In this case, the composite soaked weight percentage was 0.27%.

3. THE THIRD RESEARCH CENTER, T.R.D.I., JAPAN DEFENCE AGENCY

3.1 Preliminary Studies on Damage Tolerance Design

For the purpose of comprehending the outline of the damage tolerance design, the following preliminary studies were conducted during the period of Fiscal Year 1977 (April '77 to March '78).

(1) Fracture Toughness Test on Typical Aircraft Materials

Three specimen configurations were selected for this test program. The test results have revealed that the K_{1c} values obtained using compact tension specimens and three-point bending specimens were nearly identical, whereas those values obtained from face grooved specimens were found to be lower than the cases of the other two specimen configurations.

(2) Development of Crack Propagation Analysis

Program

The program was developed, as applicable to a number of crack configurations, by combining the crack growth laws by PARIS[4], FORMAN[5] and ISIDA, and the crack growth retardation models by WILLENBORG[6] and WHEELER[7] (Table 1).

Analyses were made, using the program, on the crack propagation under such test program as Flight-by-Flight, Low-High-Low and High-Low-High loading. The results of the analyses were, however, not found to be in good agreement with the experimental results (Fig. 20).

(3) Studies on Non-destructive Inspection

The results of applying such non-destructive inspection methods as the magnetic particle and a number of liquid penetrants obtained by a few inspectors, with varying degrees of experience, using specimens of various materials which had been treated to have artificial flaws of quenching crack, stress corrosion crack, etc., were compared with the results of microscopic inspections. While little differences were noticed between the results by inspector to inspector, or by method to method, the minimum crack length which none of inspectors allow to overlooking was determined to be 4mm.

3. 2 Full Scale Vibration and Drop Fatigue Tests on the Helicopter Type HSS-2 (Sikorsky S-61)

The objectives of these fatigue tests are to obtain technical data for the fatigue life prediction and the confirmation of the structural integrity of the aircraft.

(1) Vibration Fatigue Test

This is a computer controlled fatigue test, and is currently being run with the expected completion in June, 1979 (Fig. 21)

(2) Drop Fatigue Test

The preparation and the preliminary test run were completed in May of 1978. The plenary run of this test program is expected to resume after the completion of the vibration fatigue test.

3. 3 Fatigue Crack Propagation Studies

(1) Studies on A New Method of Crack Propagation Prevention using Artificial Wedges

Studies were made on the behavior of crack propagation when artificial wedges were inserted in fatigue cracks.

The experimental results have shown that the artificial wedges reduce the rate at which the cracks grow, and that they stop crack propagations. A new method of preventing crack propagation using artificial wedges has been proposed based on these results (Fig. 22).

(2) Experiemental Observations on the Effects of Stress Intensity Factor Range upon the Rate of Fatigue Crack Propagation

Studies on the crack propagation behavior under the $d(\Delta K)/d(2a)$, which was controlled at constant, were made using a fatigue test system with the on-line K-function control[8], with the results given as below:

a) When $d(\Delta K)/d(2a)$ is negative, the rate of crack propagation deviates from the normal curve of ΔK-da/dN, thereby showing a phenomenon of crack retardation.

b) The lower the yield stress of the material, and the greater the ΔK decreasing rate, the more prominent the crack retardation will be.

c) The following experimental equation has been obtained for the crack propagation rate under the constant $d(\Delta K)/d(2a)$:

$$\frac{d(2a)}{dN} = C\left\{\Delta K_i \, (\Delta K/\Delta K_i)^{\beta}\right\}^m \qquad (3)$$

where ΔK_i is the initial stress intensity factor range,

$$\beta = 1 \quad \text{for} \quad \frac{d(\Delta K)}{d(2a)} \geqq 0$$

$$\beta = A\sqrt{-\frac{d(\Delta K)}{d(2a)}} + 1 \quad \text{for} \quad \frac{d(\Delta K)}{d(2a)} < 0 \qquad (4)$$

A is material constant and $A = 0.167$ for HT-80 high tensile strength steel.

4. AIRCRAFT ACCIDENT INVESTIGATION COMMISSION

4. 1 Aircraft Accident Investigation in Japan

At the end of 1978, the registered aircrafts in Japan were 861 fixed wing aircrafts (including 266 air transport service), 426 helicopters and 315 gliders.

During the last five years, we had 226 aircraft accidents, involving 108 on fixed wing aircraft, 84 on helicopter and 34 on glider.

Investigation revealed that about 60% for causal factors related to pilot, 18% related to material and 22% related to weather or human factors.

Table 2 shows that the data of the accidents caused by material failure and the data in parenthesis indicates the accidents caused by fatigue. It also means that number of helicopter accident is greater than the fixed wing aircraft's and there is a trend to increase the accident caused by fatigue. The detail of the accident caused by fatigue is shown on Table 3.

5. CIVIL TRANSPORT DEVELOPMENT CORPORATION

5. 1 Japanese Work Packages in the Development of Boeing 767 Transport

The 767 (200 seater medium range transport) project marked its go-ahead in 1978. This airplane is going to be developed by Boeing under the international collaboration with Italy and Japan. The first flight of the 767 is scheduled to be in the middle part of 1981. Formal participation of Japan in the program started in October last year after signing of a contract with Boeing. Work packages allocated to Japan are forward-fuselage, mid-fuselage, aft-fuselage, wing-to-body fairing, passenger doors, cargo doors, emergency exit doors, main landing gear doors and wing ribs as illustrated in Fig. 23.

Under the contract between Boeing and Japan, Japan has conducted body splice fatigue tests and strength tests of new composite materials for wing-to-body fairing. The results of these tests are to be used in designing the 767. Under the contract, Japan has also conducted the fail-safe tests of integral skin and the high and low speed wind tunnel tests of empennage, although such are unrelated to the Japanese work packages. Japan also participates in non-work package areas such as system design/analysis, flight control technology, etc.

6. FUJI HEAVY INDUSTRIES, LTD., AIRCRAFT DIVISION

6. 1 Fatigue Tests for Model 700/710 Aircraft

Fatigue tests of Model 700/710 aircraft were terminated in April of 1978 in completion of cyclic loading enough for 80,000 flight hours fatigue life. The Model 700 is a pressurized, twin engine general usage airplane designed for certification under the N category of JCAB airworthiness regulation and FAR Part 23, and the Model 710 has the same basic airframe and systems except for power-up engines and larger gross weight. The fatigue tests conducted to evaluate the fatigue strength are as follows (Fig. 24):

(1) #02 Full Scale Fatigue Test
(2) #03 Pressurized Cabin Fatigue Test
(3) Tail Fatigue Test

The #02 full scale fatigue test is a spectrum testing with a complete primary structure, in which flight-by-flight load sequence with five types of programmed flight cycles is adopted to take account of the combined effects of flight load, pressurization load and ground load. The flight loads spectrum was constructed in a combination of the gust and maneuver load spectra specified by FAA (AFS-120-73-2), and was sliced in six load levels to construct the test load spectrum (Fig. 25). The detail of #02 test method had already been informed at the 15th ICAF meeting held in Darmstadt, Gemany on May 9 ~ 13, 1977.

The #03 pressurized cabin fatigue test was conducted in order to make early detecion of serious fatigue damages on the pressurized cabin structure expected to have more damages than the wing and associated structure, and in order to reflect the structural modification for the defects on production type aircraft. In this test, only cyclic pressurization load, 0 to 5.9 psi, was applied on the cabin structure.

The tail fatigue test was put in operation in order to evaluate the fatigue strength of empennage structure under tail buffet load in stall condition, which was anticipated to be severe enough to result in structural damage. The empennage structure of #03 pressurized cabin fatigue test article was used as the test article of this test (Fig. 24). The tail buffet load spectra represented by cumulative frequency of horizonta-tail rolling moment were derived from the data accumulated through the 187 times stall practices during flight load survey (Fig. 26). The test load spectrum was set so as to cover the severest buffet load of Model 710 original horizontal-tail configuration and the sequence of load was low-high-low of six load levels within each block.

The loading in vibratory condition was generated

by the exciting instrument. The exciting force was applied through one batter board installed on the right hand side of horizontal stabilizer and the frequency of empennage vibration was set near the actual tail buffet frequency of 8 Hz by adjusting the quantity of balance weights of five batter boards on horizontal and vertical stabilizers.

Fig. 27 shows the progress of fatigue tests. The #02 test was continued up to 80,256 flight hours fatigue life. It took just two years from May of 1976 to April of 1978. The #03 test took about seven months from January to August of 1977 to get 84,364 flight hours. The tail test took two months from September to November of 1977 to get 585 blocks.

The occurrence of fatigue damages in #02 full scale fatigue test is shown in Fig. 28. The total number of fatigue damages was 135 including minor damages which have no effect on fatigue strength. 97 items out of the 135 damages occurred on the pressurized cabin structure and the rest on the wing and associated structure. The #03 pressurized cabin fatigue test had 58 damages. The decrease in occurrence of fatigue damages in comparison with the number of damages on #02 cabin structure can be considered due to contribution of the structural improvement on #03 test article. The total number of damages in tail fatigue test was 22. The major part of damages was fastener failure of horizontal-tail supporting fittings and vertical-tail root fittings such as head-off of bolt or loosing of rivet.

Based on the evaluation of the #02 and #03 test results, following service lives were established with scatter factor 4:

16,500 flight hours for Model 700

14,500 flight hours for Model 710

For tail buffet, based on the tail fatigue test result and reduction of the buffet load due to modification of horizontal-tail configuration made for improvement of stall characteristics of Model 710 (Fig. 26), the following allowable number of times in stall practice were derived with scatter factor 4:

670,000 times for mild buffet of Model 700

32,200 times for mild buffet of Model 710

7. MITSUBISHI HEAVY INDUSTRIES, LTD., AIRCRAFT WORKS

7.1 Study on Fractography of Fatigue for Ultra-high Strength Steels

Preliminary study was made for the purpose of estimating the stress intensity factor ΔK and fatigue crack growth rate, da/dN on the basis of fractography of ultra-high strength steels, 4330V and 300M.

As the results, ΔK and da/dN were related to the striation pitch, p and the mixture ratio of fracture modes which were observed on the fracture surface. From these relationship, it may be possible to quantitatively analyze fatigue failures for ultra-high strength steels.

7.2 A Method for Fatigue Crack Growth Analysis

In order to investigate the crack growth retardation effects of aluminum alloy sheets, two stage cyclic loading tests were carried out, and the effects of cyclic number of the first stage overloading were determined.

The quantiy of retardation increased with the cyclic number n, and saturated in a given cyclic number n_{sl}. The saturation cyclic number n_{sl} is shown by the following equation:

$$n_{sl} = \frac{\alpha \cdot \gamma_{yl}}{\left(\frac{da}{dN}\right)_1} \qquad (5)$$

where α is experimental constant, γ_{yl} and $\left(\frac{da}{dN}\right)_1$ are the plastic region size and the crack growth rate by the first stage loading stress just before the second stage, respectively.

On the basis of these test results, computer calculation program was made to analyze fatigue crack growth.

7.3 Application Research of Carbon Composite Material to Airframe Structures

By carbon composite material, tensile and bending fatigue tests were carried out with sheets, sandwich constructions, beam structures and joint structures of hinge component with both adhesion and rivet fastening.

From these test results, the fatigue strength of laminated material was evaluated.

8. KAWASAKI HEAVY INDUSTRIES, LTD., AIRCRAFT GROUP

8.1 Fatigue Strength of GFRP and CFRP Lugs

To invesigate the strength of GFRP and CFRP in jointed portion, the wrap around lugs were fatigue tested. Materials of the lugs were glass roving-epoxy, carbon roving-epoxy and combined carbon and glass roving-epoxy. Alternating tensions were loaded through two pins.

The test results of the GFRP lugs are shown in Fig. 29. Failures were coupled shear failure with fiber failure at pin attached surface.

The results of tests were:

(1) The strength was highly dependent on D/W (pin diameter -lug width ratio), whose trend was analogous with those of metal lugs.

(2) Carbon roving lugs showed the highest strength in the tests and combined carbon and glass lugs showed the intermediate strength between carbon and glass lugs.

These lugs were analyzed using finite element method and the results are shown in Fig. 30. The correlation between analysis and test results was very good.

8.2 Surface Strength of GFRP Bars

As a part of our program to study the fretting characteristics of composite materials, GFRP rectangular bars supported at two points were fatigue tested to investigate the influence of the materials which were in contact with them.

Several metals, platings and plastics were tested as supporting materials. Test results of titanium alloy and TFE (tetra-fluoro-ethylene) cloth are shown in Fig. 31. In case of titanium alloy, the failure occurred at the point of contact. It was initially the shear failure and then the micro bucklings of fibers followed.

The TFE cloth bonded to the metal was the best among the tested materials and there were no failures at the point of contact.

The shear failures occurred in the middle layer of the bars along the neutral plane.

8.3 Effects of Heat Treatment on Fatigue Strength of Ti-6A1-4V Alloys

To investigate the relation between the microstructure and fatigue strength of Ti-6A1-4 alloy, fatigue tests were conducted using the Schenk type plane bending fatigue testing machine with four kinds of differently heat treated specimens (Table 4). And the fatigue loads were applied under conditions of the three different stress ratios, R = -1, 0 and 0.5.

It was found that the microstructure, especially the size and configuration of α-phase, has a great effect on the fatigue strength and tensile ductility, but no effect on other mechanical properties. Especially, it is remarkable that fatigue strength at 10^7 cycles is higher for the granular α-phase than for the acicular α-phase at the stress ratio R = -1, but it is opposite at R = 0.5.

9. ACKNOWLEDGEMENT

The authors wish to express their sincerest gratitude for Dr. L. E. Jarfall and Mr. A. Maenhaut in cordially inviting Japan to the 16th ICAF Meeting as a guest and granting a precious opportunity to review the recent aeronautical fatigue investigations in Japan. They also earnestly desire to be able to have such opportunity in the future in order to exchange useful informations on aeronautical fatigue.

Finally, they greatly appreciate the cooperation and assistance of Professor T. Yokobori and other members of the Sixth Sub-committee on Aeronautical Fatigue of the Japan Society for Promotion of Sciences.

10. REFERENCES

1) T. Kamiyama et al.; Review of Aeronautical Fatigue Investigations in Japan 1975-1977, the 5th ICAF Meeting, 1977

2) R. Steiner; A Review of NASA High-altitude Clear Air Turbulence Sampling Programs, AIAA Paper No. 65-13, 1965

3) Military Specification, Airplane Strength and Rigidity Reliability Requirements, MIL A-8866 (ASG) 18, 1960

4) P. C. Paris et al.; Trans. ASME, Ser. D 85-4, 1963

5) R. G. Forman et al.; Trans. ASME, Ser. 893, 1967

6) J. D. Willenborg et al.; AFFDL-TM-71-1-FBR, 1971

7) O. E. Wheeler; Trans. ASME, J. Basic Engineer-

ing, Vol. 94, Ser. D. No. 1, 1972

8) H. Kitagawa et al.; Proc. 2nd ICM, Boston, 1976

ICAF Documents

983) K. Yamane et al.; Operation Experiences Related to Severe Turbulence between September 1973 and August 1975, NAL TM-319, 1976

984) Y. Naito et al.; Fatigue Crack Propagation under Program Loads, Joint JSME-ASME Applied Mechanics Western Conference, 1975

985) Y. Kawada; On the Relation between the Probability of Failure and the Factor of Safety in the Design of Machine Parts under Repeated Load, Bulletin of the JSME, Vol. 20, No. 142, 1977

986) H. Kobayashi et al.; A Fractographic Study on Evaluation of Fracture Toughness, Fracture 1977, Vol. 3, ICF 4, Waterloo, Canada, 1977

987) E. Sasaki et al.; Fatigue Crack Propagation Rate and Stress Intensity Threshold Level of Several Structural Materials at Varying Stress Ratios ($-1 \sim 0.8$), Trans. National Research Institute for Metals, Japan Vol. 19, No. 4, 1977

988) H. Nishitani et al.; Influence of Mean Stress on Crack Closure Phenomenon and Fatigue Crack Propagation, Bulletin of the JSME, Vol. 20, No. 141, 1977

989) K. Ogura et al.; Influence of Mechanical Factors on the Fatigue Crack Closure, Fracture 1977, Vol. 2, ICF 4, Waterloo, Canada, 1977

990) T. Tanaka et al.; Studies on Fatigue Damage Caused by Stresses below the Endurance Limit, Bulletin of the JSME, Vol. 20, No. 143, 1977

991) T. Sakai et al.; Fatigue Crack Initiation in 18% Ni Maraging Steel and Its Propagation Behavior in Early Stage, Proc. 20th Japan Congress of Materials Reserach, 1977

992) T. Tanimoto et al.; Static and Fatigue Properties of Carbon Fiber Reinforced Plastics, Proc. the 2nd Int. Conf. on Mechanical Behavior of Materials, 1976

993) K. Nishioka et al.; Fatigue Crack Propagation Behaviors of Various Steels, The Sumitomo Search, No. 7, 1977

994) H. Nakamura et al.; An Experimental of the Estimation of Corrosion Fatigue Strength, Technical Papers, Bulletin of the MESJ, Vol. 5, No. 3, 1977

1069) Shimokawa et al.; Relationship between Scatter of Fatigue Life and S-N Curve of 2024-T3 Aircraft Structural Aluminium Alloy Specimen with a Sharp Notch ($K_t = 8.25$) under a Constant Temperature and Humidity Condition, NAL TR-412T, 1977

1070) T. Shimokawa; A New Plotting Method of Estimate the Population Parameters of the Normal Distribution, NAL TR-464T, 1977

1071) A. Kobayashi et al.; Prefatigue Hysteresis Effects on Viscoelastic Crack Propagation, J. Applied Polymer Science, Vol. 21, 1977

1072) K. Tanaka et al.; A Tentative Explanation for Two Parameters, C and m, in Paris Equation of Fatigue Crack Growth, Int. J. Fracture, Vol. 13, No. 5, 1977

1073) S. Matsuoka et al.; Delayed Retardation Phenomenon of Fatigue Crack Growth resulting from a Single Application of Overload, Engng Fracture Mechanics, Vol. 10, 1978

1074) K. Endo et al.; Effects of Environment on Fretting Fatigue, Wear, 48, 1978

1075) M. Kikukawa et al.; Fatigue Crack Closure Behavior at Low Stress Intensity Level, Proc. 2nd ICM, Boston, Special Volume, 1976

1076) M. Kikukawa et al.; Fatigue Crack Propagation and Closure Behavior under Plane Strain Condition, Int. J. Fracture, 13, 1977

1077) T. Nakagawa et al.; Prediction of Miner Damage Distribution by Bayesian Method, Proc. HOPE Int. JSME Symp., 1977

1078) H. Nishitani; Stress Concentration for the Tension of a Strip with Edge Cracks or Elliptic Arc Notches, Proc. 1st Int. Conf. on Numerical Methods in Fracture Mechanics, Swansea, 1978

1079) H. Anzai et al.; The On-site Indication of Fatigue Damage under Complex Load by using a Micor-computer, Proc. Int. Conf. on Application of Computers in Fatigue, Soc. of Environmental Engnrs Fatigue Group, 1978

Table 1 Contents of the Program for Prediction of a Crack Propagation

		Contents
Input data		(1) load sequence (2) choice of crack propagation equation (3) crack shape (4) choice of retardation model
Output data		a-N curve and a-N data
ANALYSIS FUNCTION	Equation for crack propagation	(1) PARIS (2) FORMAN (3) ISIDA
	Crack configulation	(1) surface flaw (2) center crack of plate (3) crack located between stringers (4) crack located at stringer position (5) integral skin (strip, ISIDA's solution) (6) a-ΔK data
	Retardation model	(1) WILLENBORG (2) WHEELER

Table 2 Material Failure Accident

A/C Type \ Failure Part	Airframe					Power Plant	Total
	Propeller or Rotor	Tail Section	Landing System	Control System	Other		
Fixed Wing	(3)	0	3+(3)	1	1	3+(1)	8+(7)
Helicopter	(2)	(2)	0	5+(3)	3	5+(3)	13+(10)
Total	(5)	(2)	3+(3)	6+(3)	4	8+(4)	21+(17)

Table 3 Fatigue Accident

Part	Date	Type	Origin of Fatigue
Propeller or Rotor	14 Jul. '73	Bell 47G	Rear edge on fitting parts of tail rotor blade
	3 Nov. '73	C 206F	Stress concentration at screw parts of No.2 propeller blade
	6 Mar. '75	FA 200	Stress concentration at screw parts of No.2 propeller hub
	10 Nov. '75	FA 200	Stone-pit at backside of propeller blade edge
	25 Jul. '77	HU 369	Pitting corrosion at tail rotor hub (Maraging steel)
Helicopter	21 Feb. '74	HU 269	Pitting corrosion at cluster fitting of center frame
	15 Jul. '75	HU 269	Stress concentration at fitting metal and rivet of horizontal stabilizer
	11 Feb. '77	Bell 204	Stress concentration at fitting flange of vertical fin
	21 Jul. '77	SA 316	Stress concentration at flange on coupling shaft of engine
	9 Aug. '77	Bell 47G	Pitting corrosion at support parts of torque tube assembly
Engine	17 Sep. '75	B 727	Pratt & Whitney JT8D-9A, Pitting corrosion at wedding parts (Ps 4) of combustion chamber outcase
	26 Jan. '76	HU 369	Allison 250-C18A, Pitting corrosion at 3rd stage compressor blade
	2 Aug. '76	HU 269	Lycoming HIO-360-D/A, Stress concentration at exhaust valve of No.2 cylinder
	22 Aug. '77	HU 369	Allison 250-C18A, Pitting corrosion at 3rd stage compressor blade
Landing Gear System	29 Sep. '74	Aero Com.	Wheel rim of nose landing gear
	13 Oct. '75	C 402	Stress concentration at side link support rib of left landing gear
	7 Oct. '76	C 402	Stress concentration at torque arm support bracket of nose landing gear

Table 4 Heat Treatment of Specimens

Mill Anneal	As Recieved Condition (820°C × 15 min. and Air Cool)
Duplex Anneal	954°C × 30 min., Air Cool and 704°C × 4 hr., Air Cool
Recrystallization Anneal	927°C × 4 hr., Furnace Cool to 760°C and Air Cool to Room Temperature
Beta Anneal	1038°C × 30 min., Air Cool and 704°C × 4 hr., Air Cool

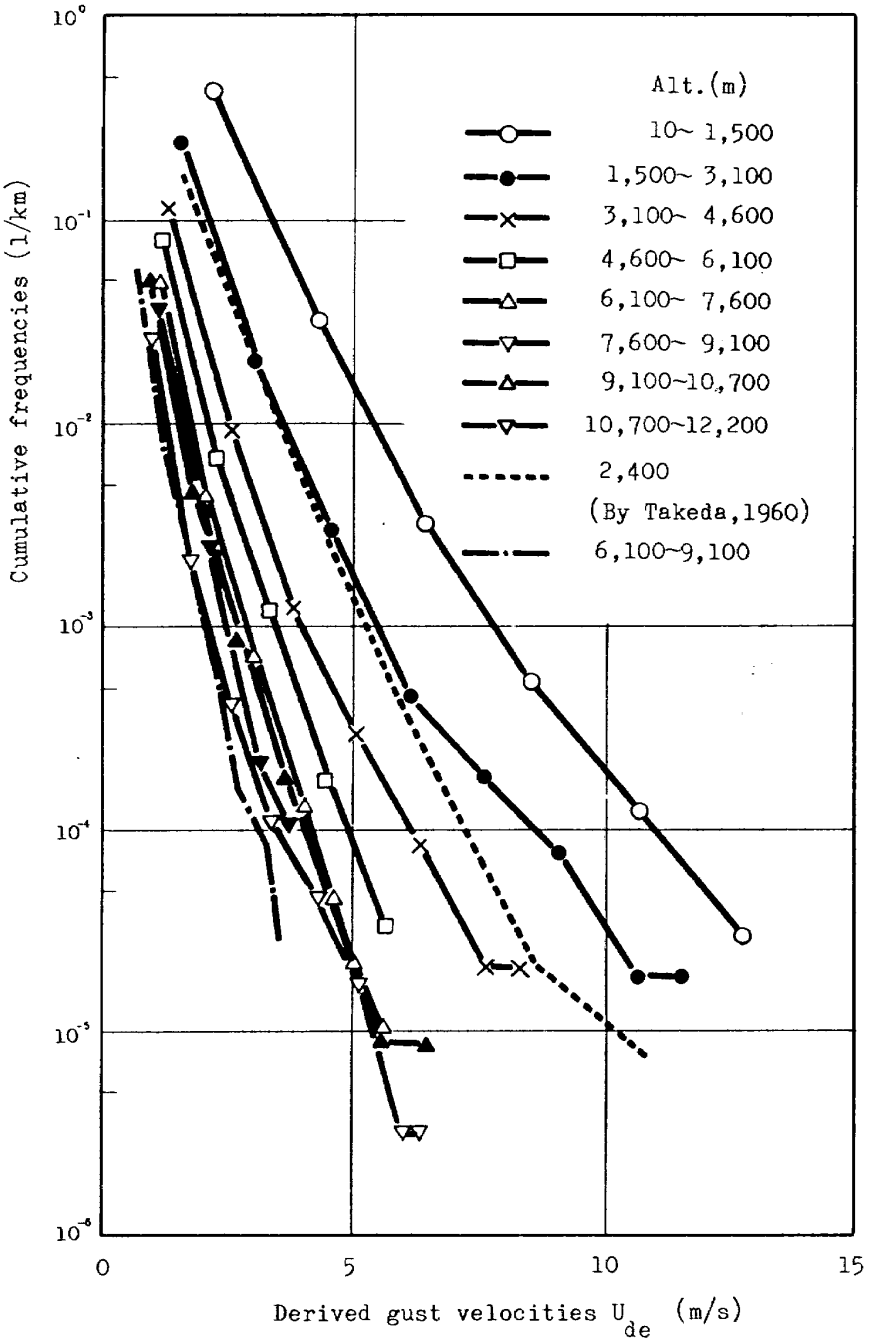

Fig. 1 Frequencies Distributions of Gust Velocities

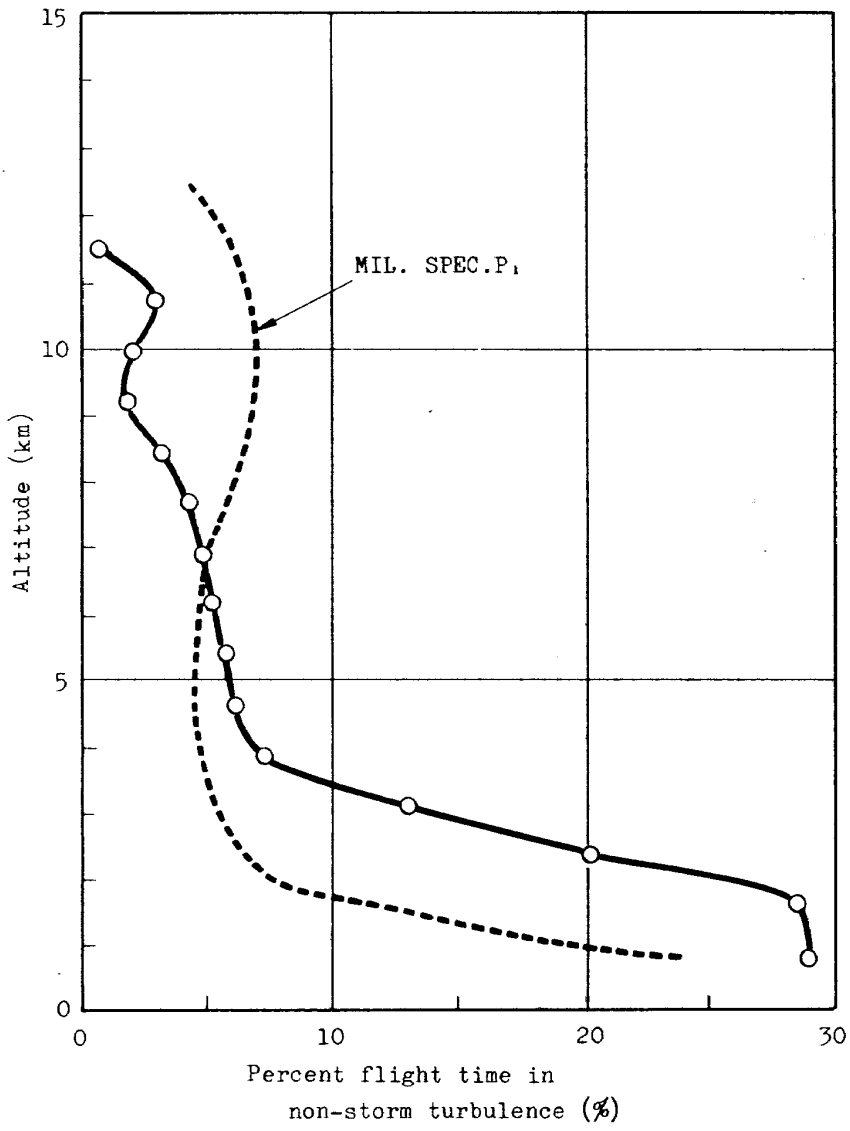

Fig. 2 Proportion of Flight Time in Non-storm Turbulence

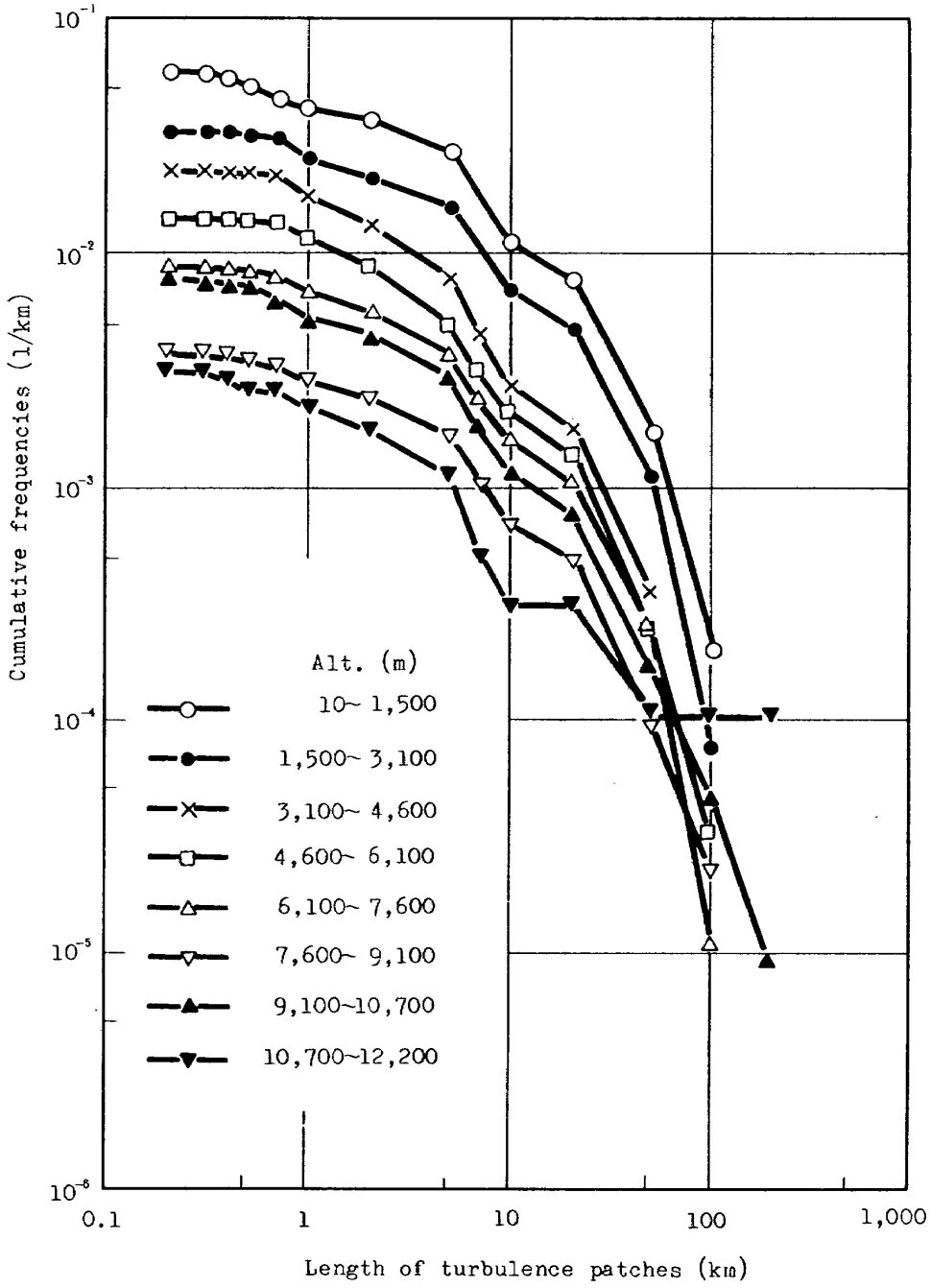

Fig. 3 Frequencies Distributions of the Length of Turbulence Patches

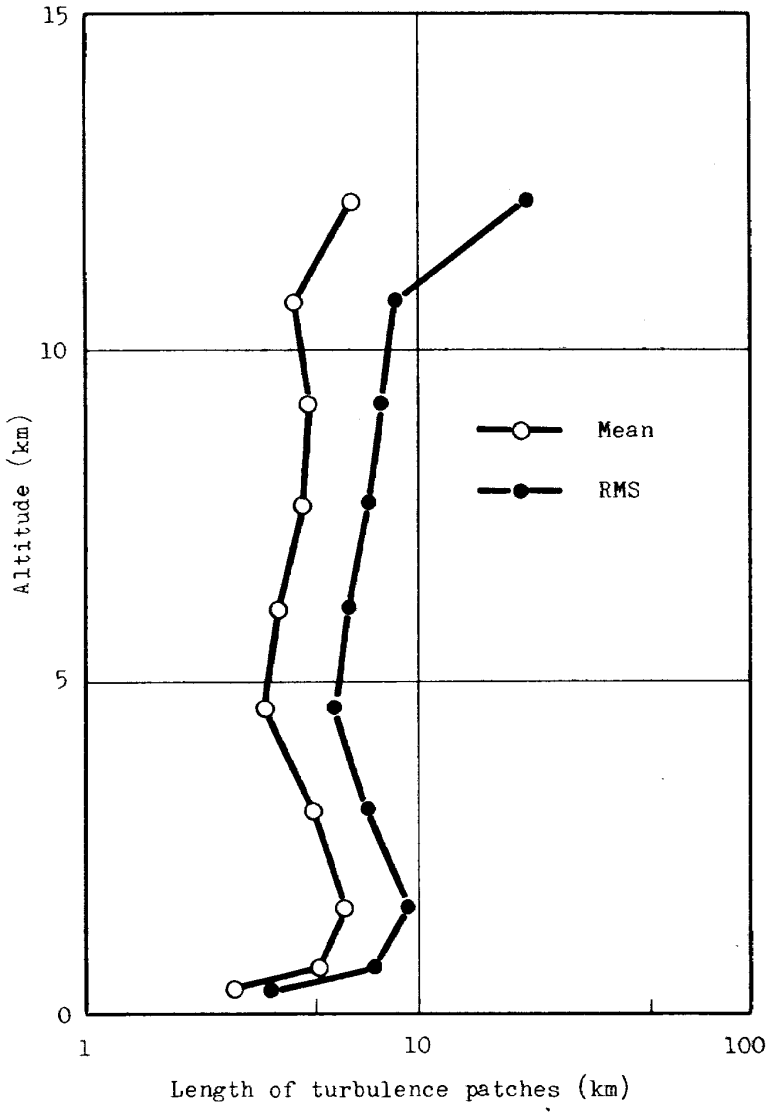

Fig. 4 Variation of the Length of Turbulence Patches with Altitude

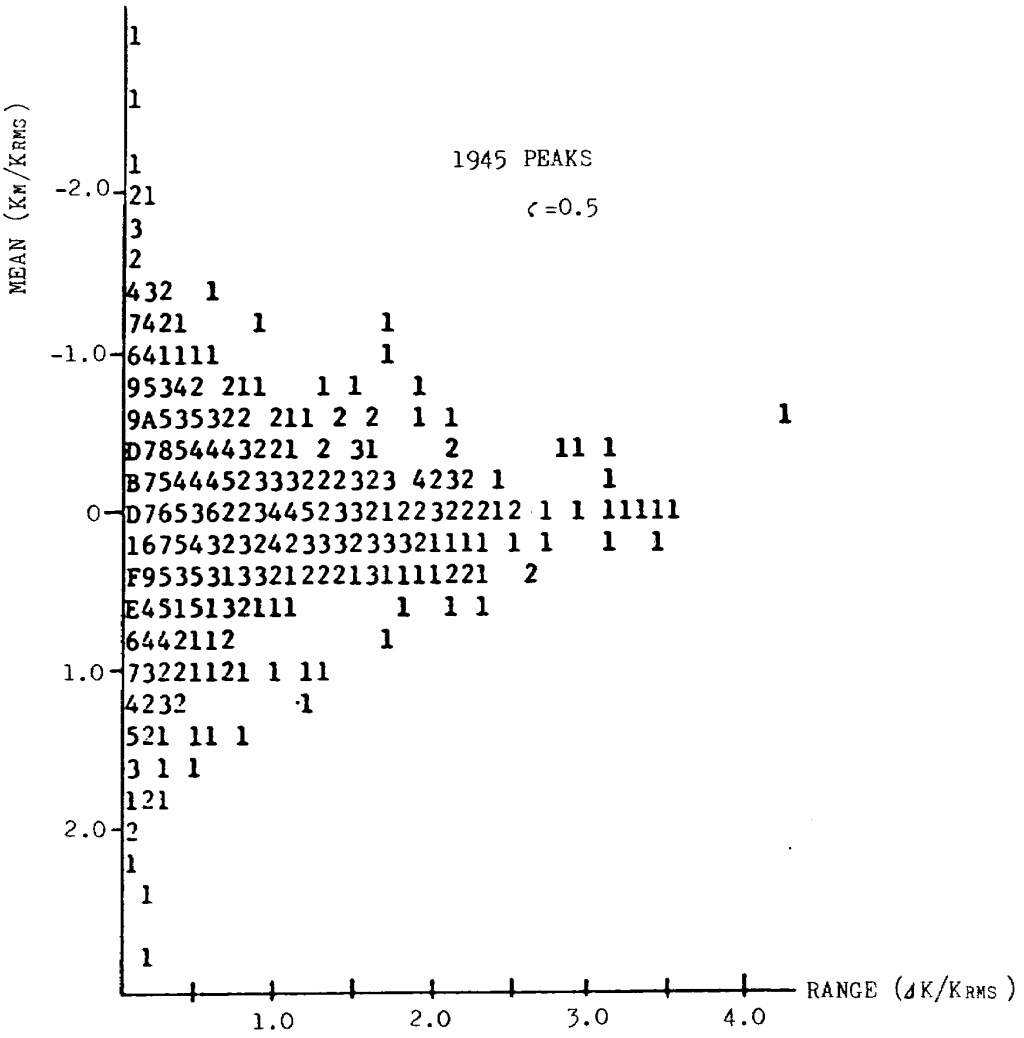

Fig. 5 Joint Distribution of ΔK and Km

Notes: (1) Krms means the root mean square value of the time history of K.
(2) The value in the table denotes the frequency distribution in 0.5% unit and (A, B, C, ---) means (10, 11, 12, ---).

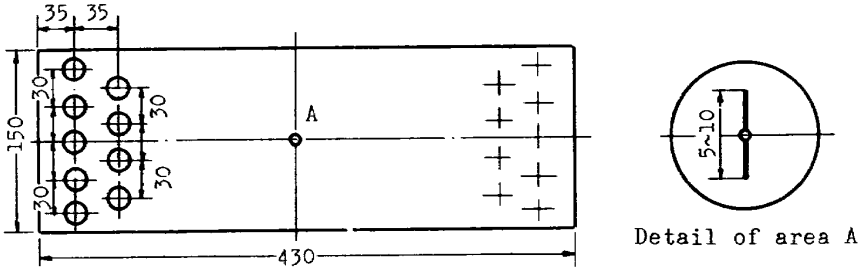

Fig. 6 The Center-cracked Strip Specimen

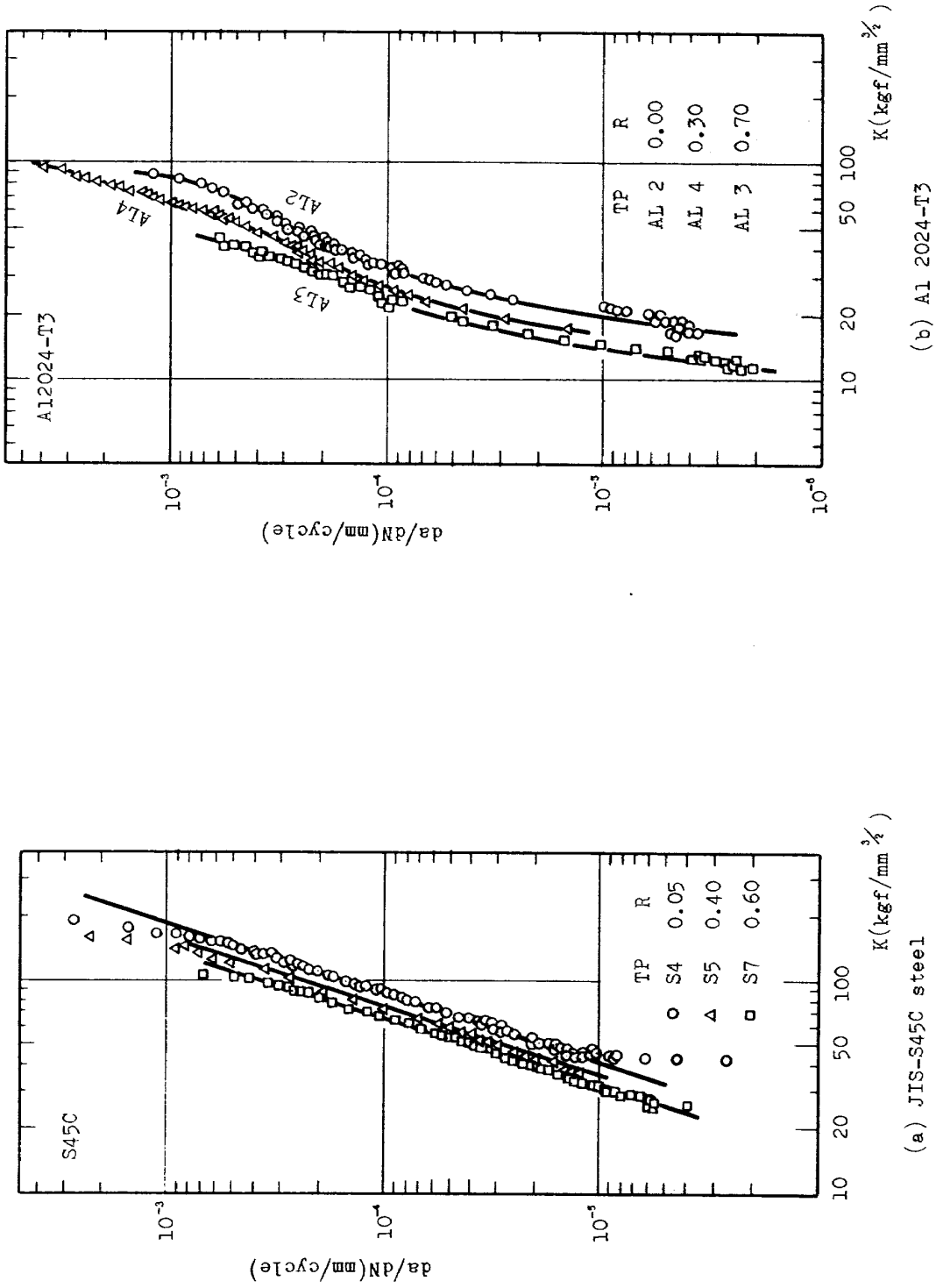

(a) JIS-S45C steel

(b) Al 2024-T3

Fig. 7 Fatigue Crack Growth Rates under Constant Amplitude Load

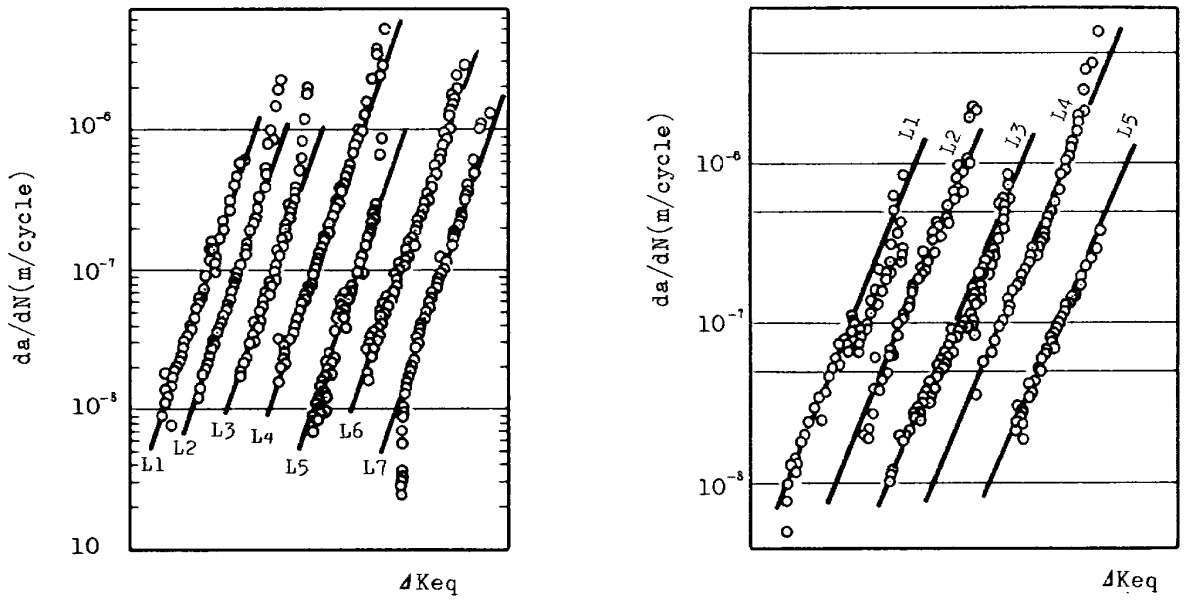

(a) JIS-S45C steel (b) Al 2024-T3

Fig. 8 Prediction of Crack Growth Rates by the HL Method

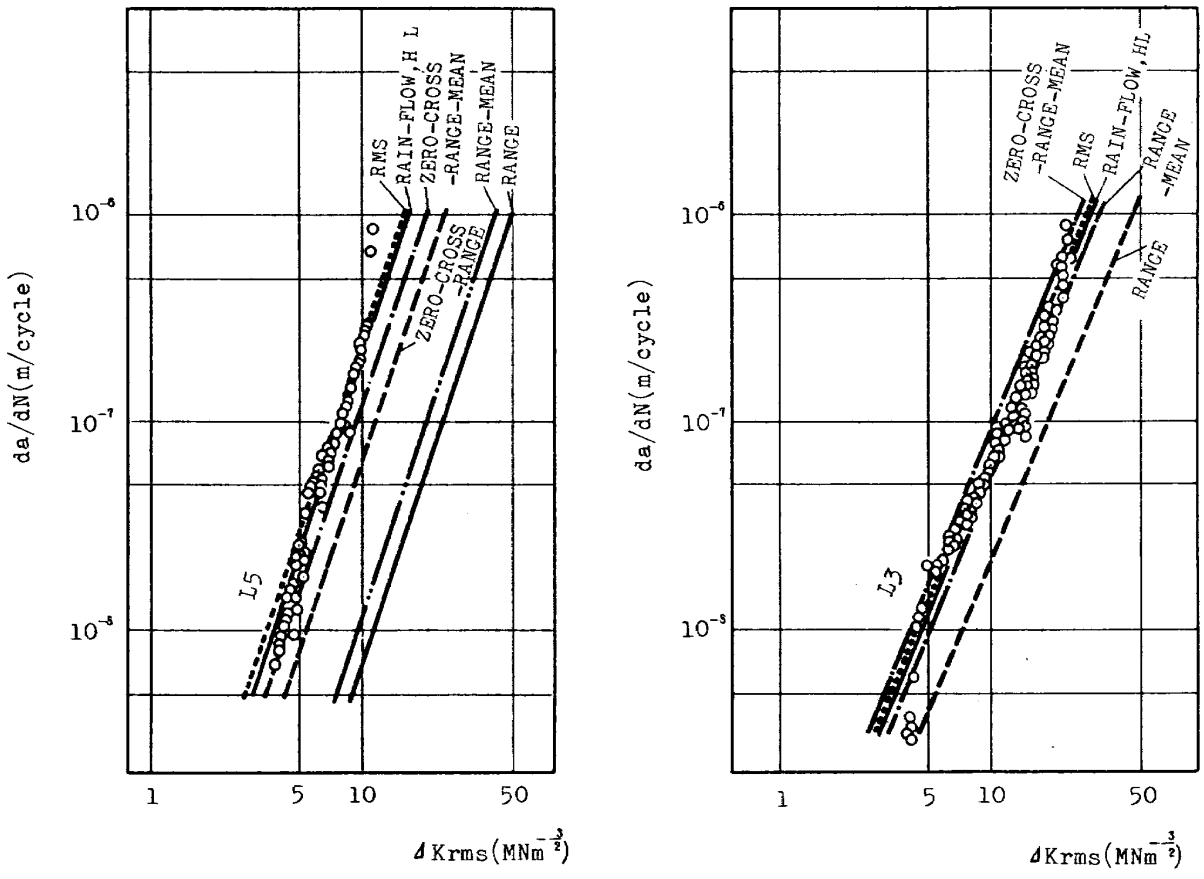

(a) JIS-S45C steel (b) Al 2024-T3

Fig. 9 Comparison among Several Counting Methods

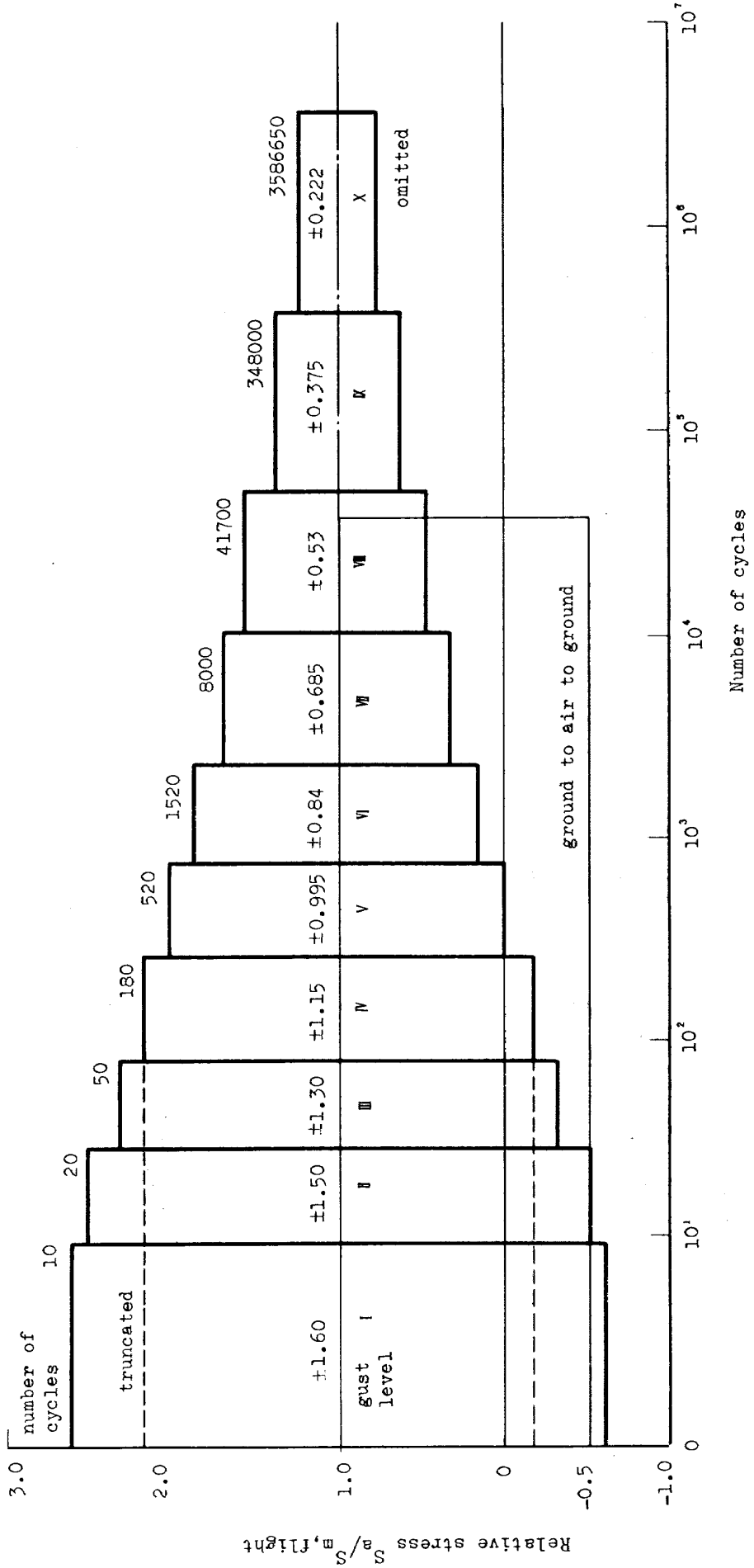

Fig. 10 Test Load Spectrum for 40,000 Flights

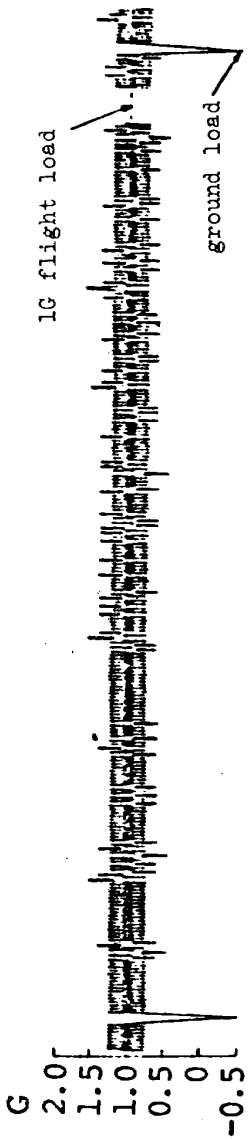

Fig. 11 An Example of the Standardized Load Sequence

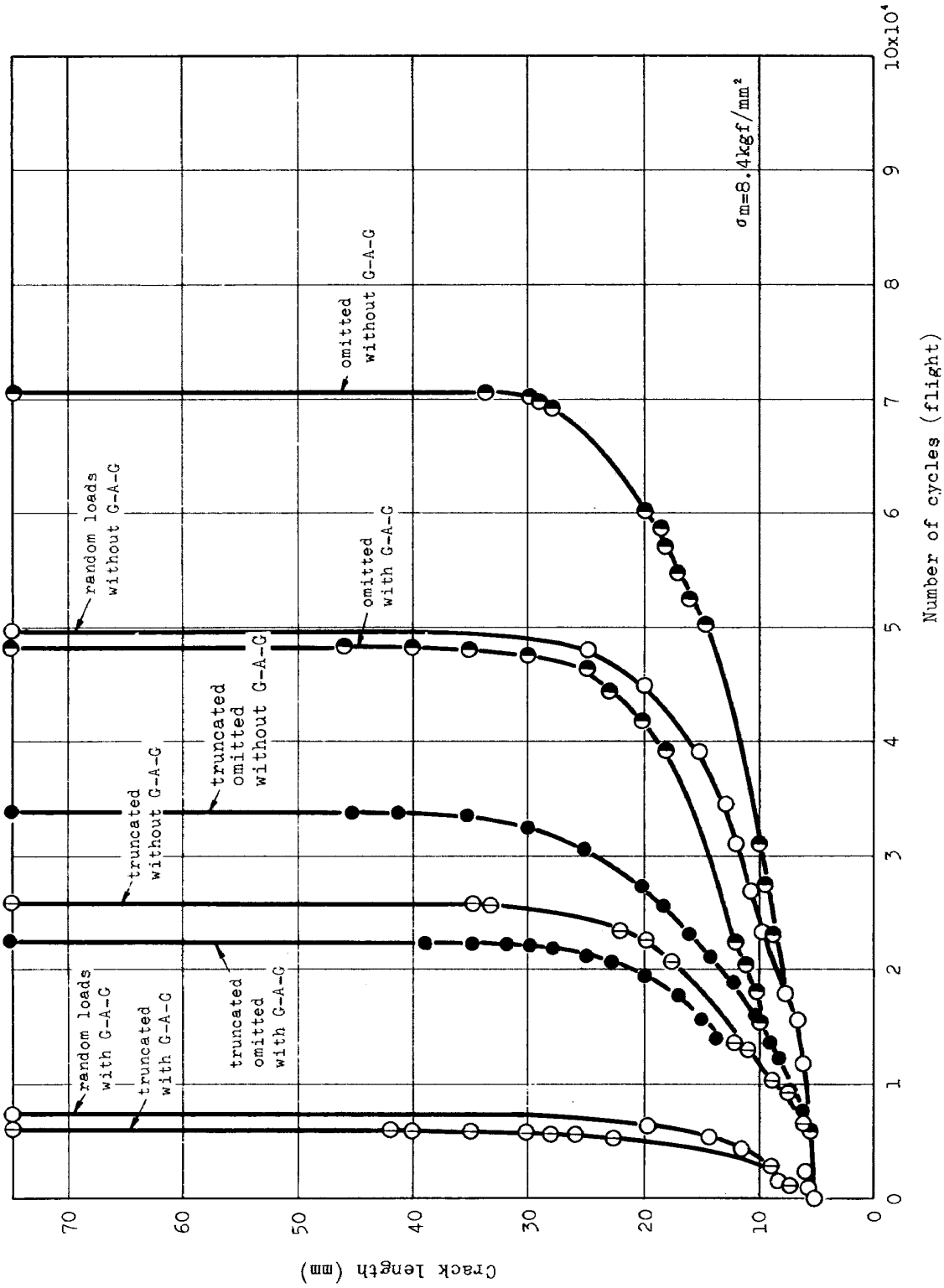

Fig. 12 Comparison of Test Results

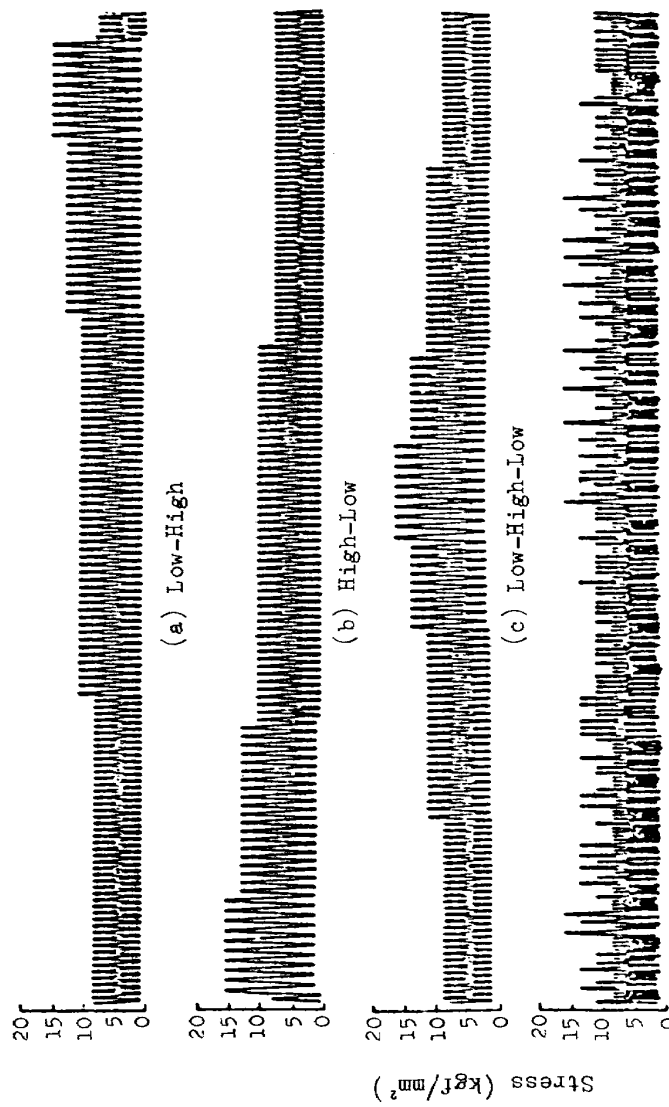

Fig. 13 Example of Test Loads

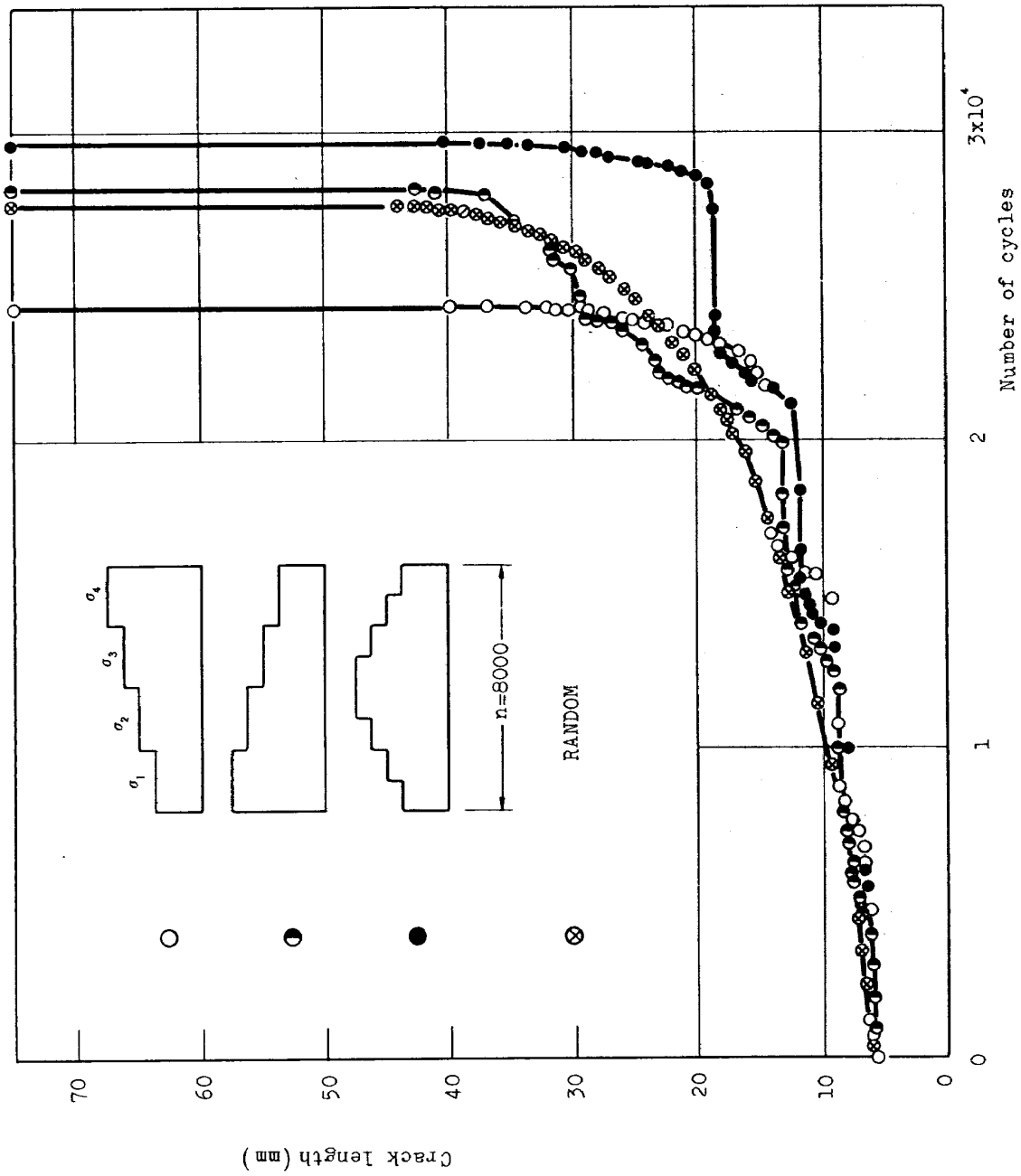

Fig. 14 Comparison of Test Results

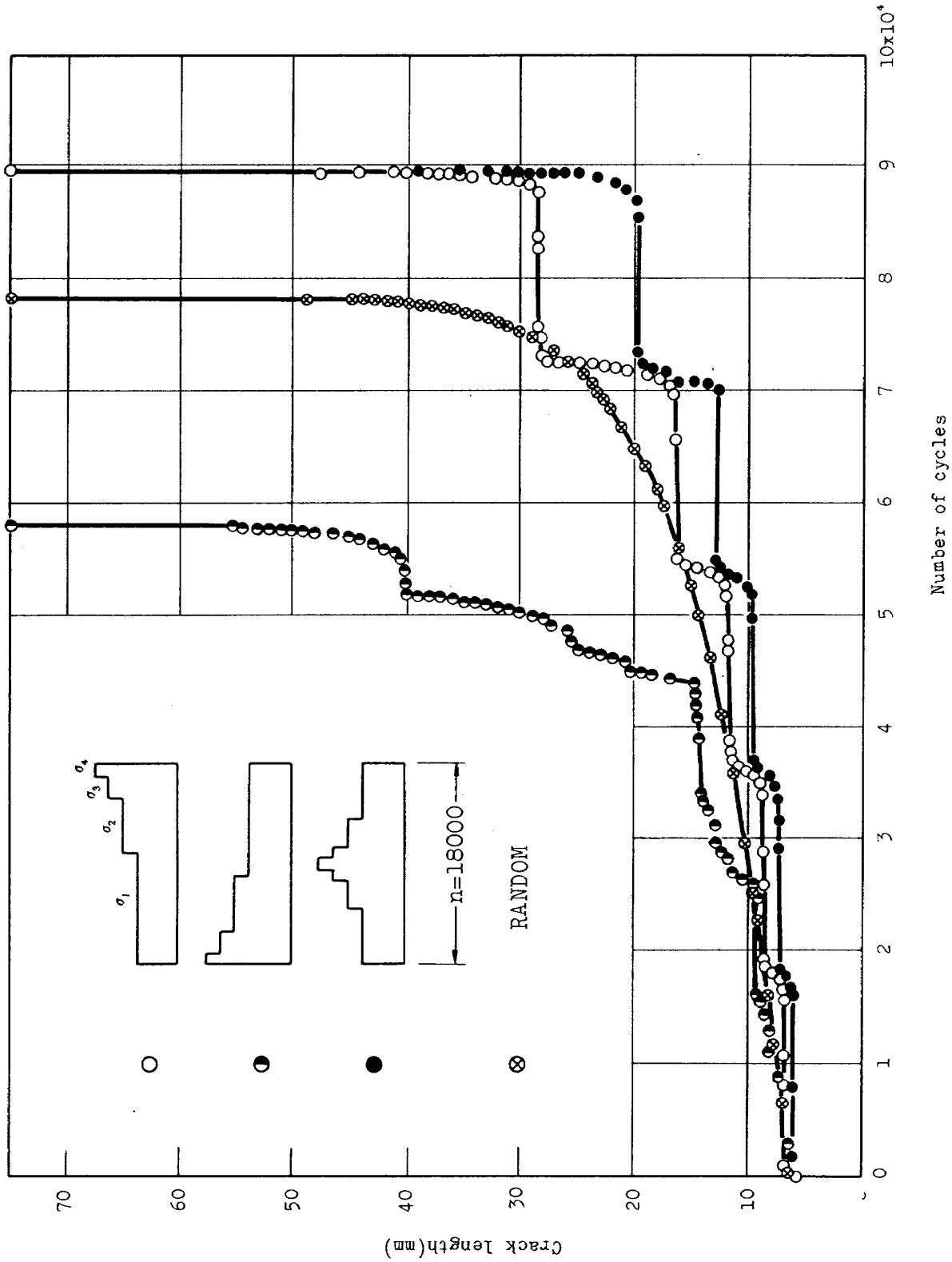

Fig. 15 Comparison of Test Results

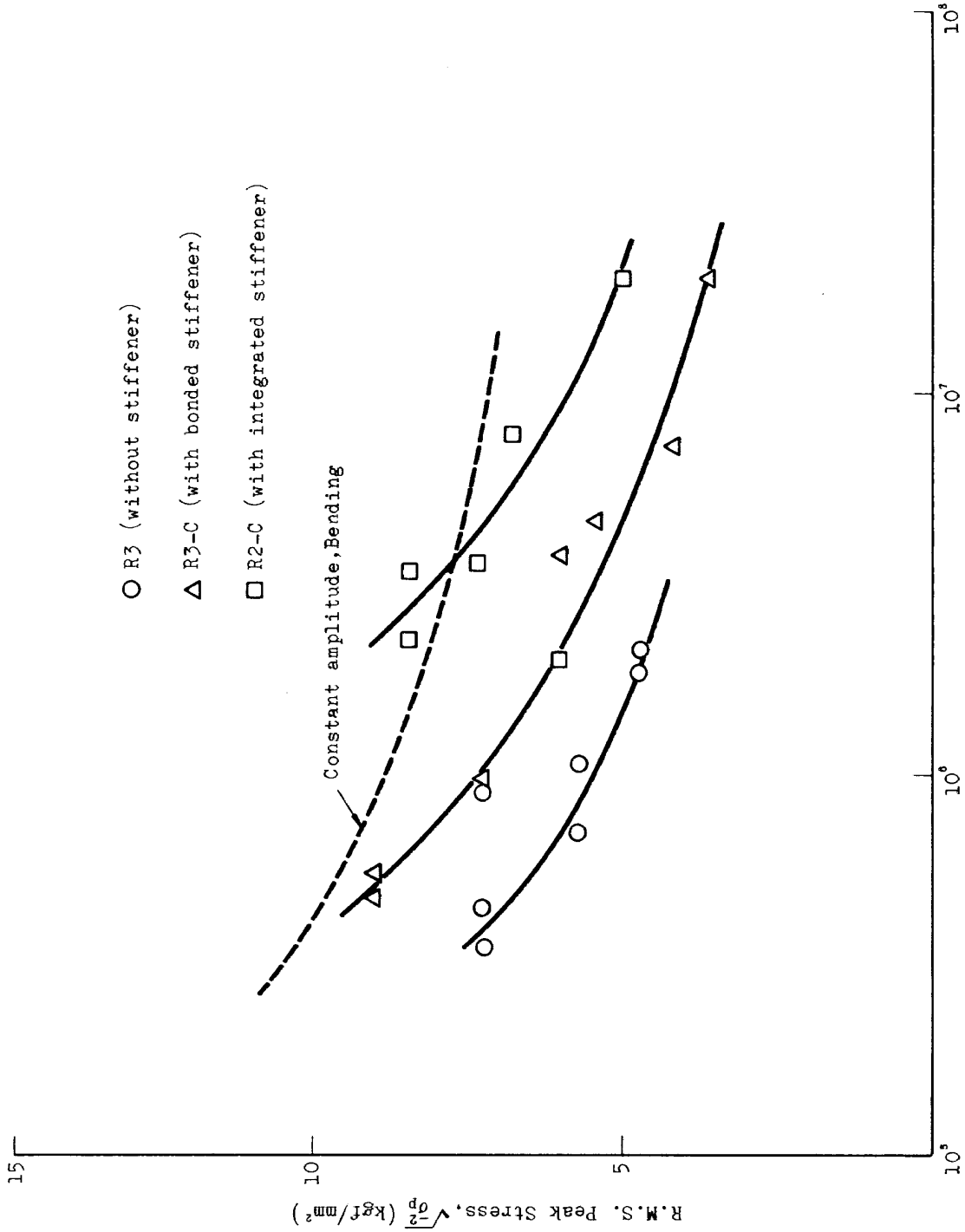

Fig. 16 Equivalent S-N Curves of GFRP Panels under Acoustic Loading

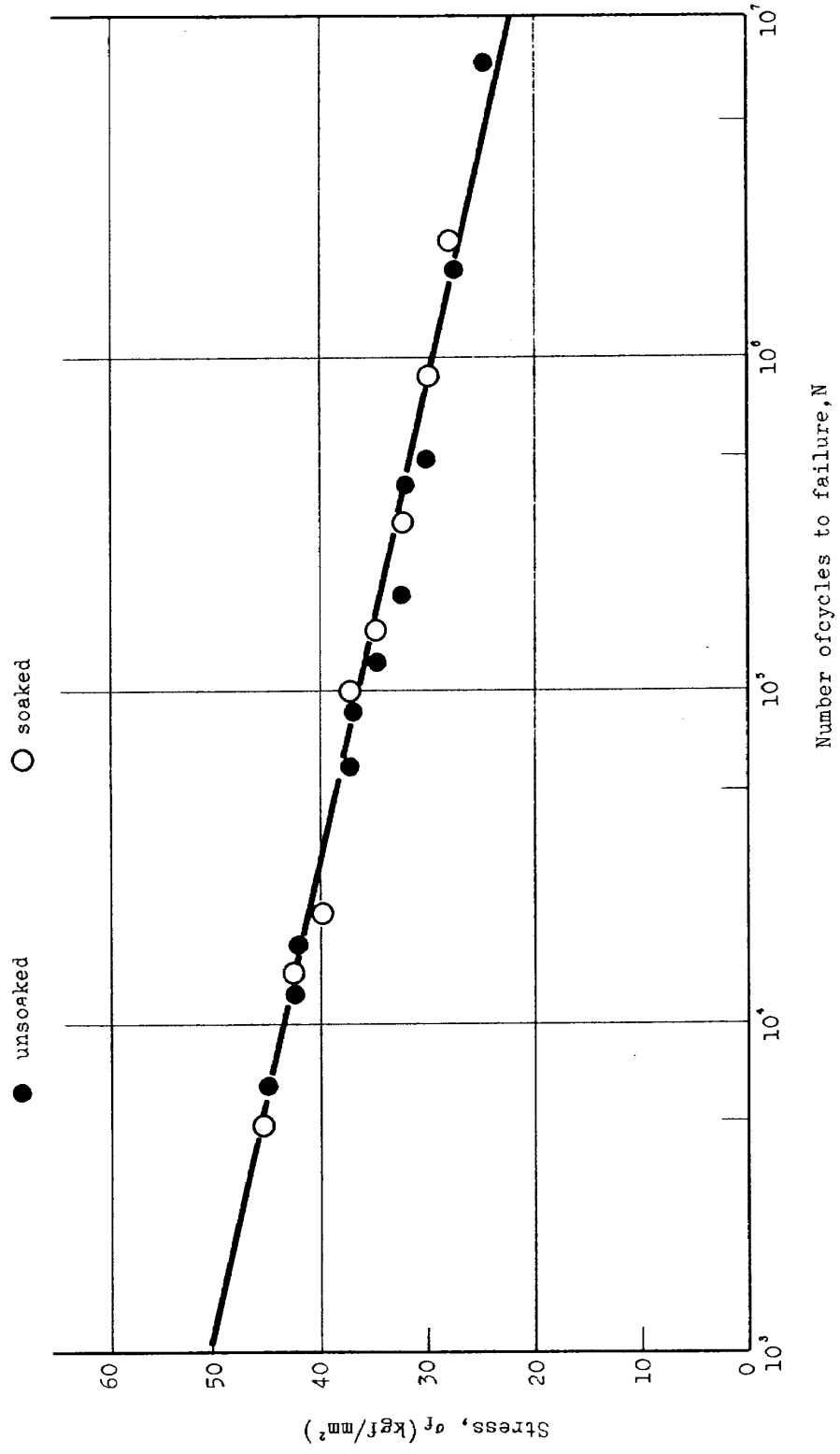

Fig. 17 S-N Curve for XAS/MRX-3501 (0°, +45°, 90°) 24-ply, Composite Soaked Weight Percentage 0.24%

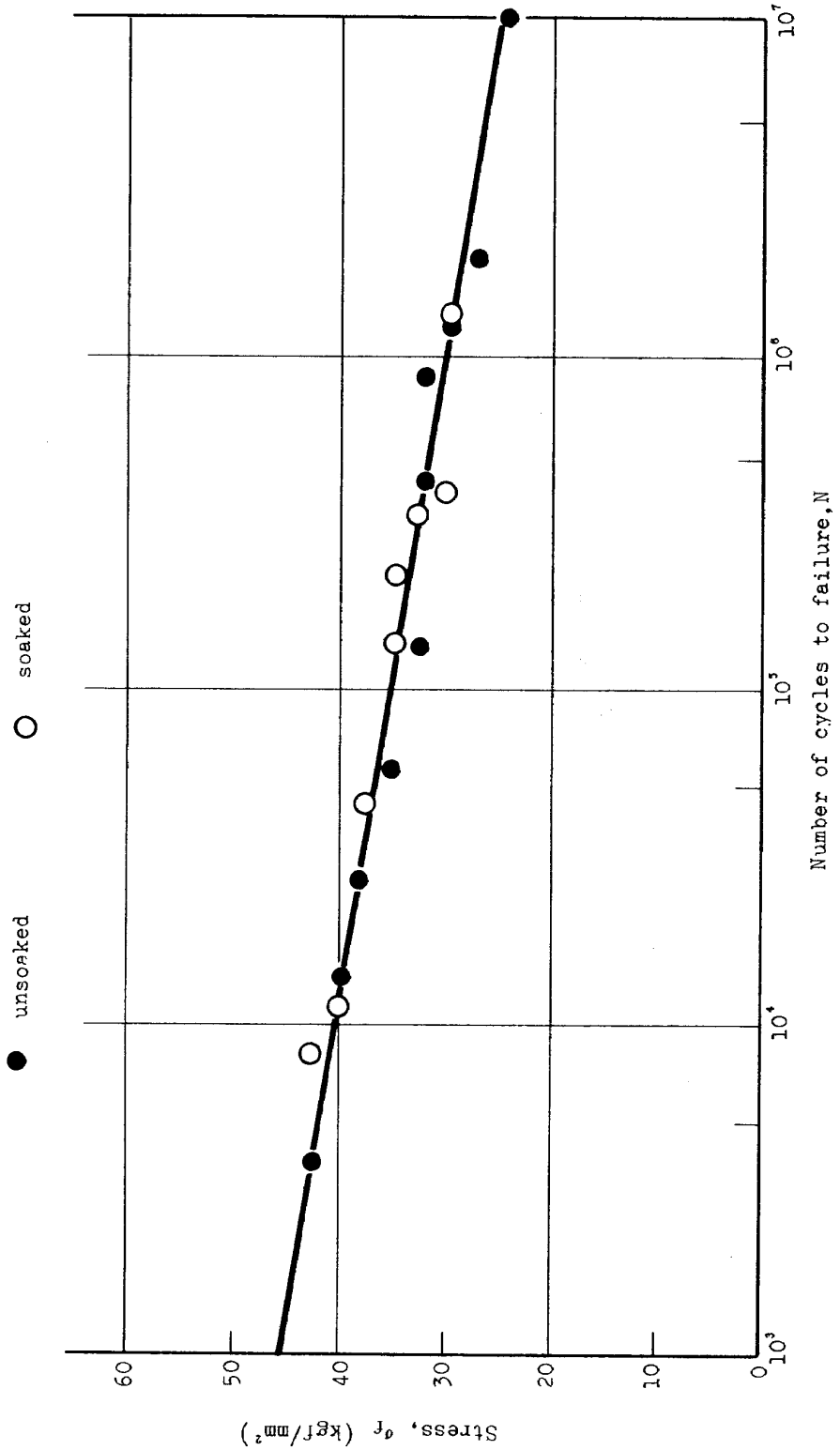

Fig. 18 S-N Cuve for Z-3/#241 (0°, +45°, 90°) 24-ply, Composite Soaked Weight Percentage 0.24%

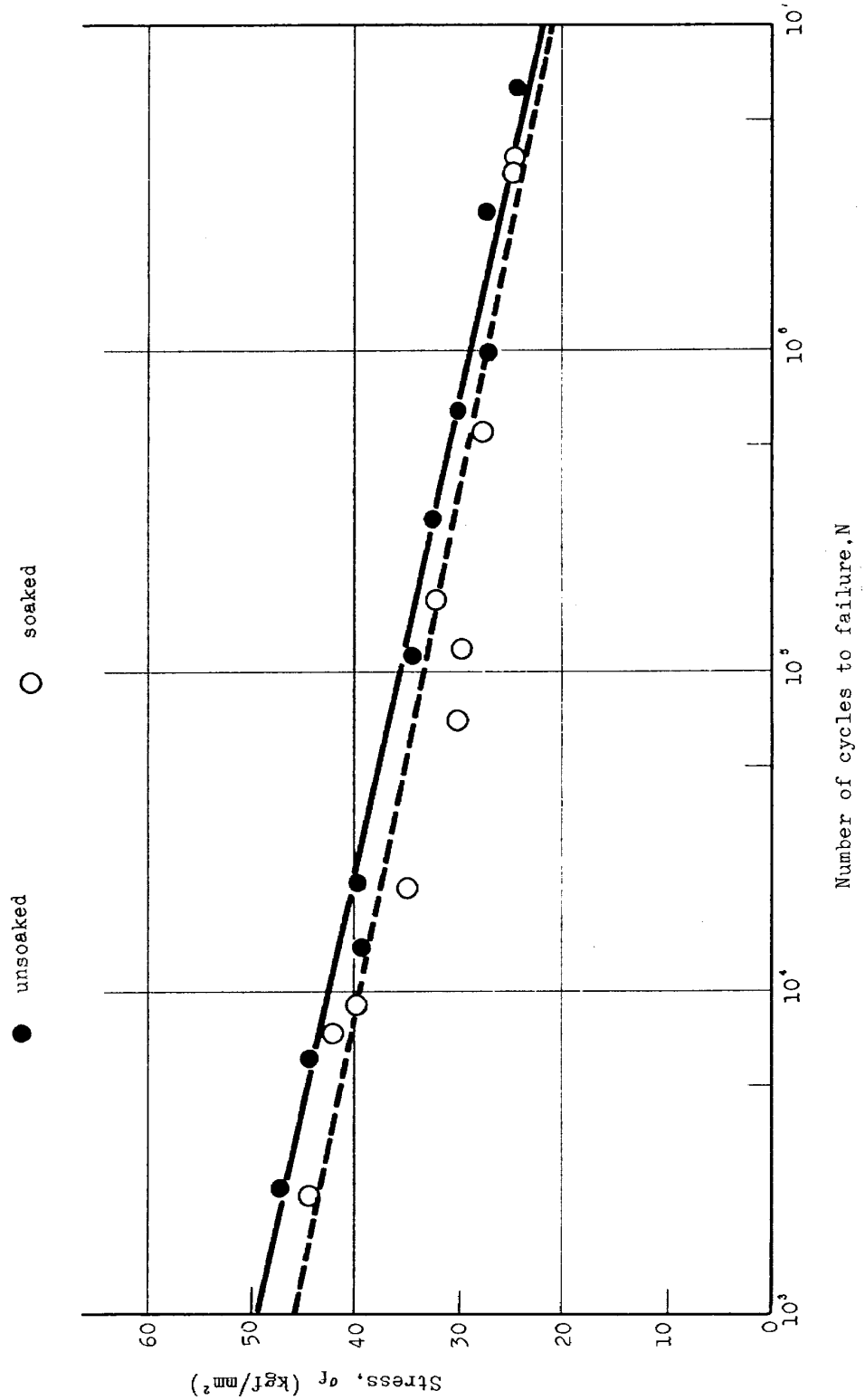

Fig. 19 S-N Curve for T-300/#3130 (0°, +45°, 90°) 24-ply, Composite Soaked Weight Percentage 0.27%

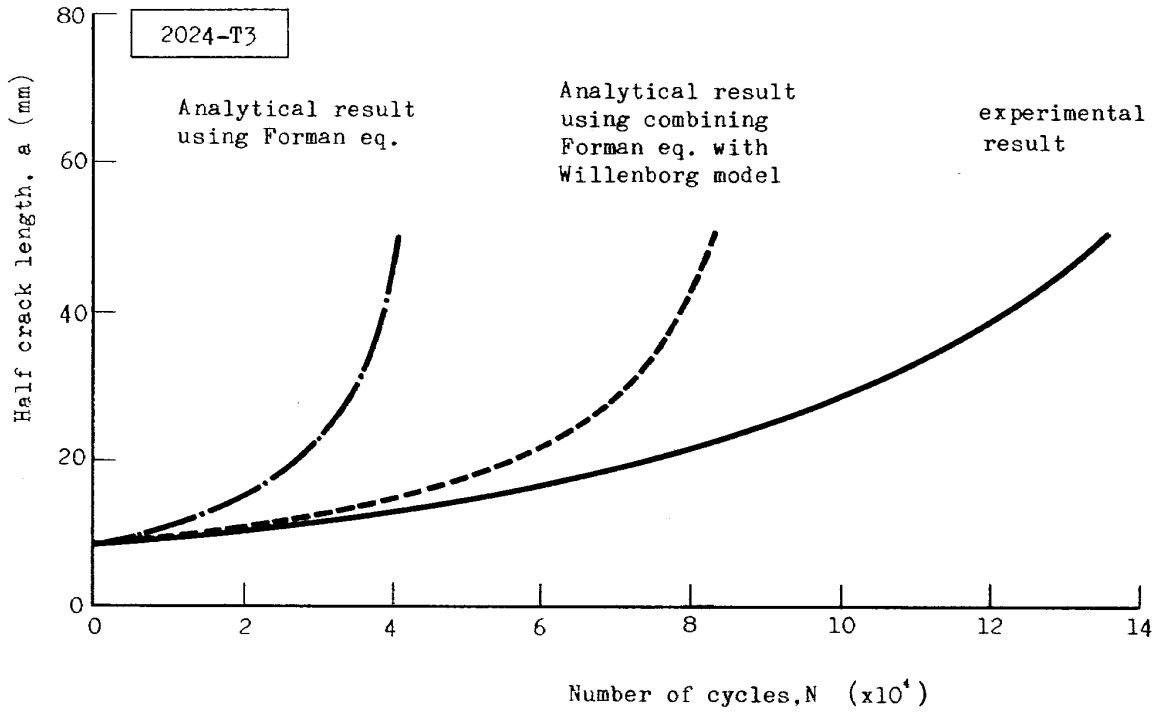

Fig. 20 An Example of a-N Curve Comparison between Analytical and Experimental Results Tested by Flight-by-Flight Program

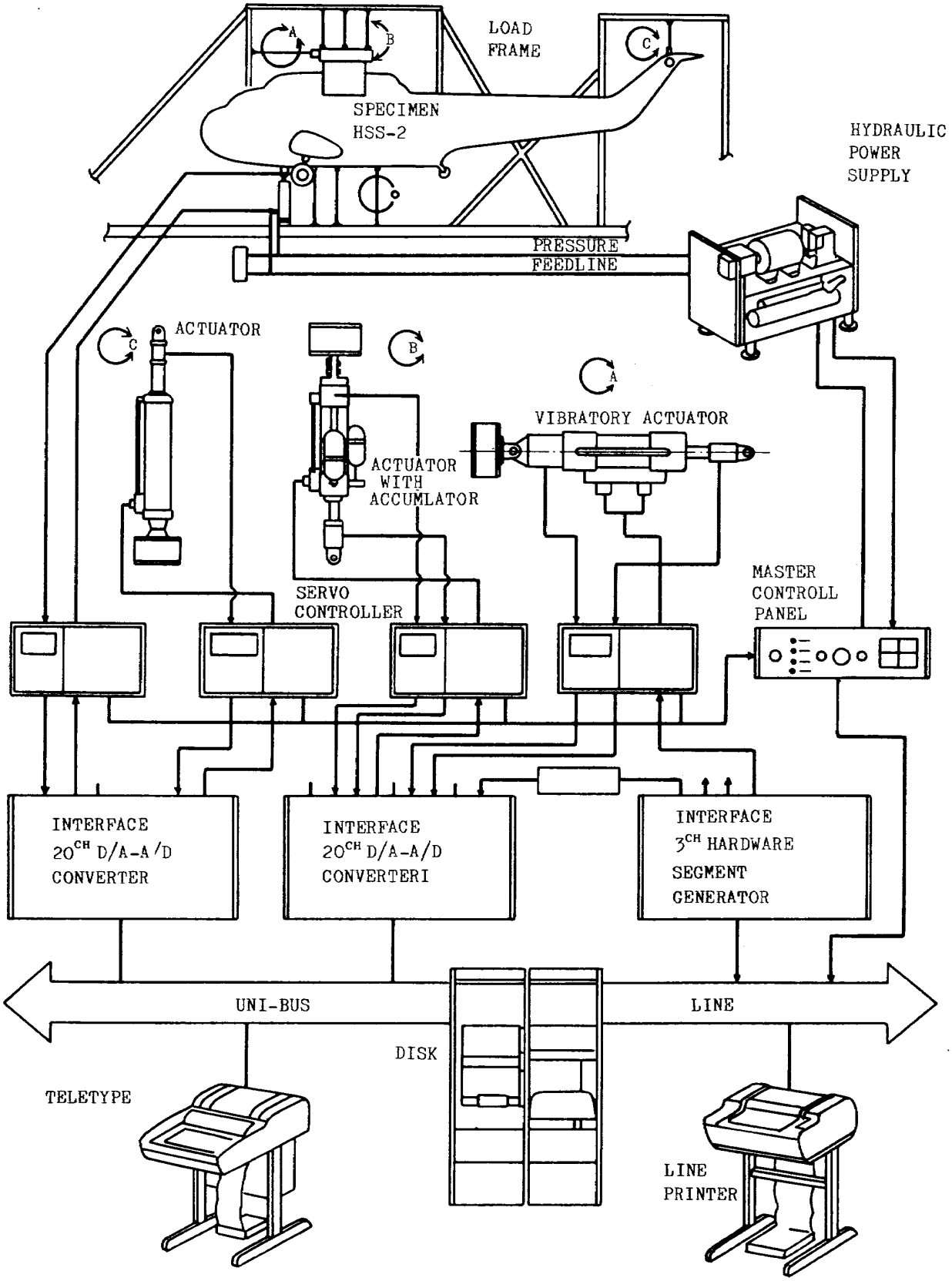

Fig. 21 Vibration Fatigue Testing System Scheme

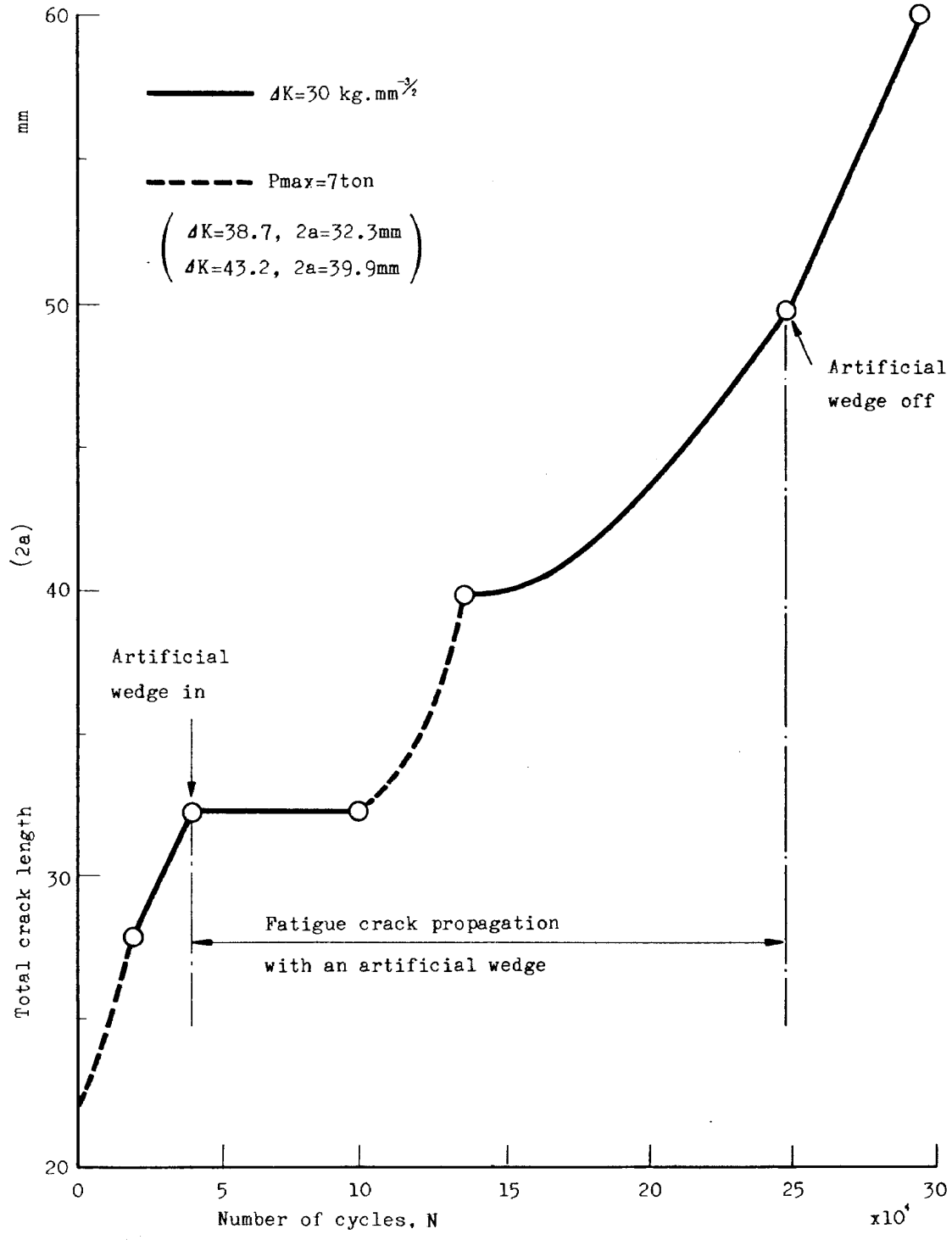

Fig. 22 An a-N Curve by a Fatigue Crack Propagation Test with and without an Artificial Wedge in the Crack

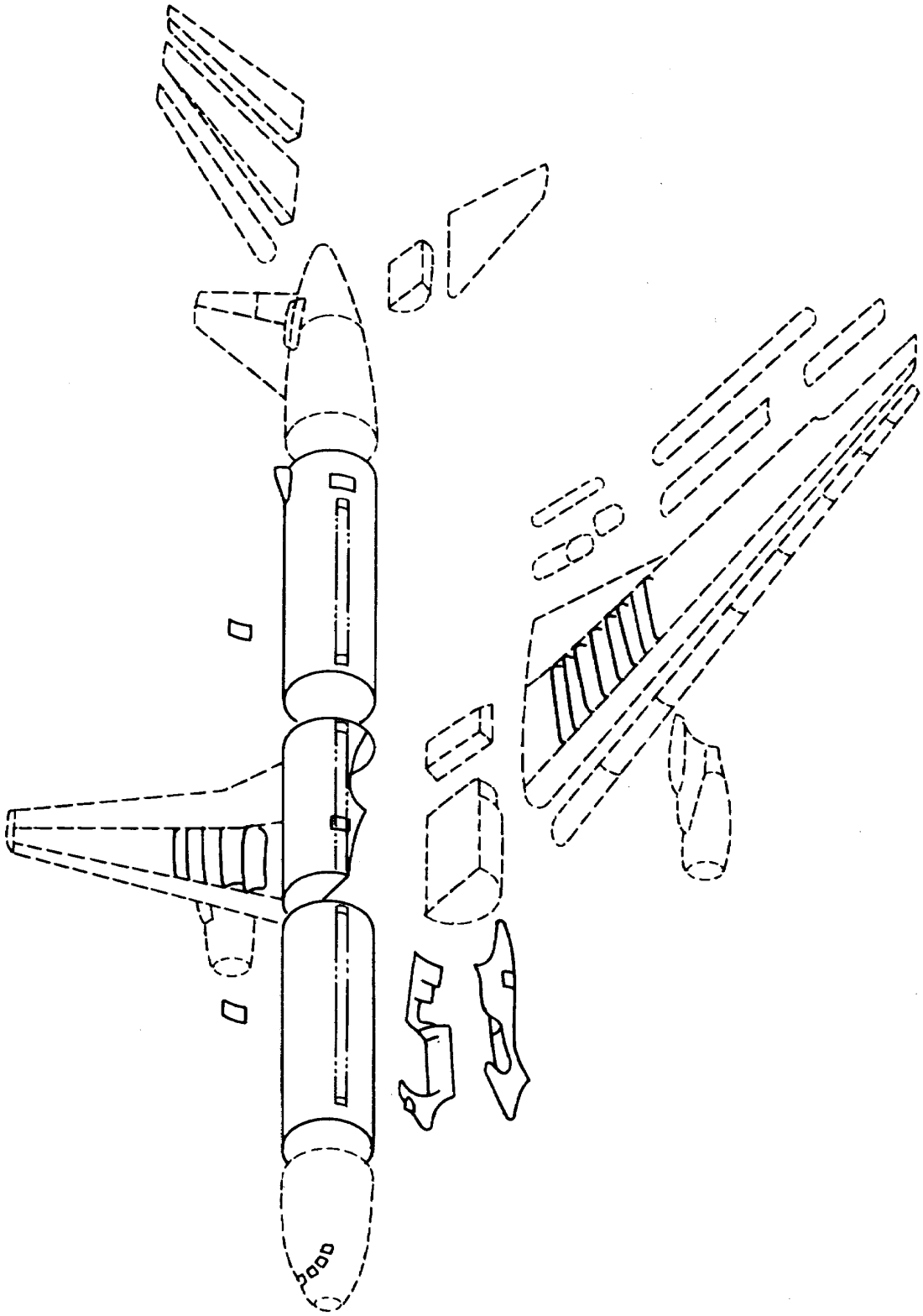

Fig. 23 Work Packages Allocated to Japan in the Development of Boeing 767
(Solid Line shows the Japanese Work Packages)

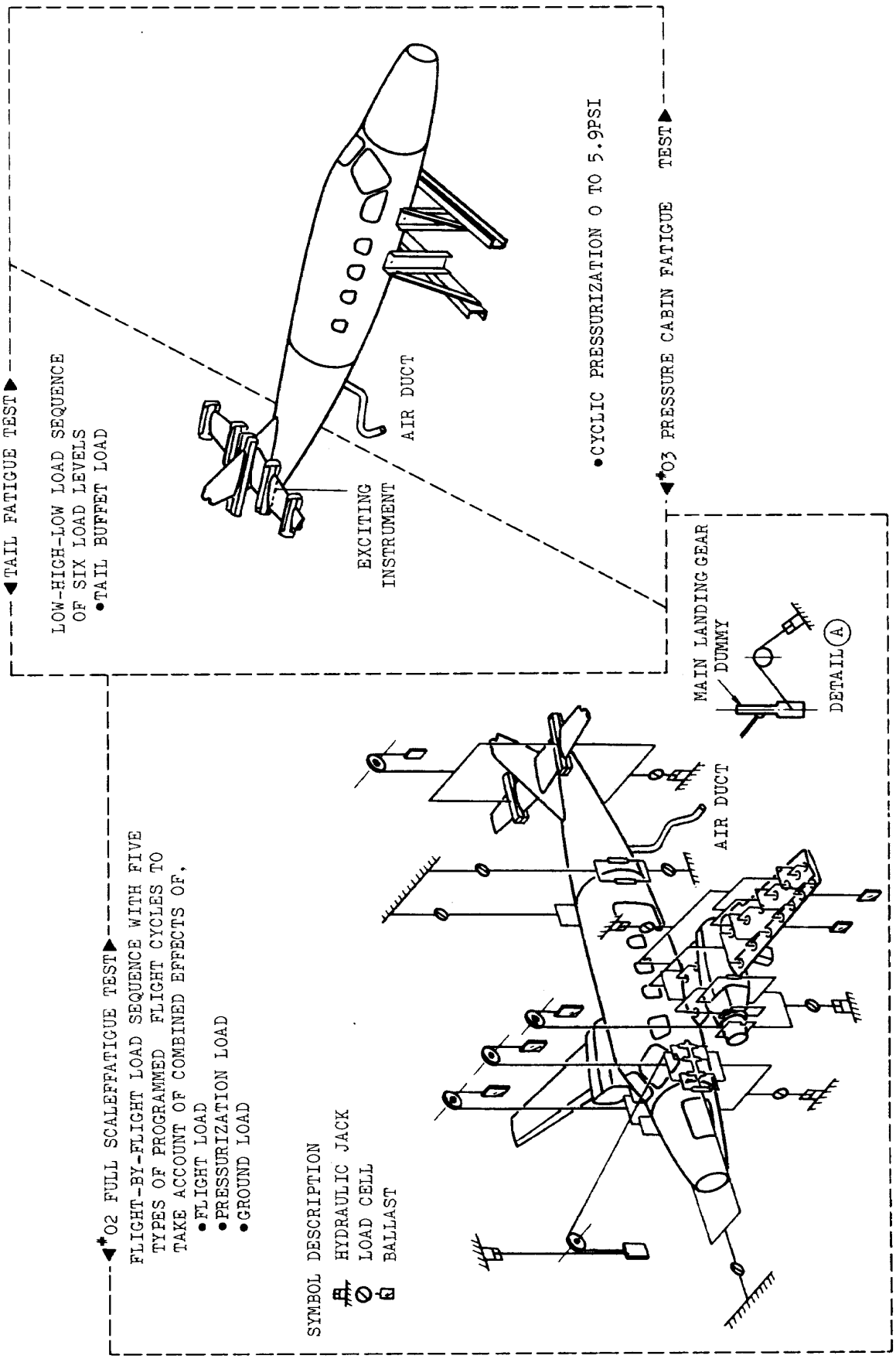

Fig. 24 Summary of the Fatigue Tests

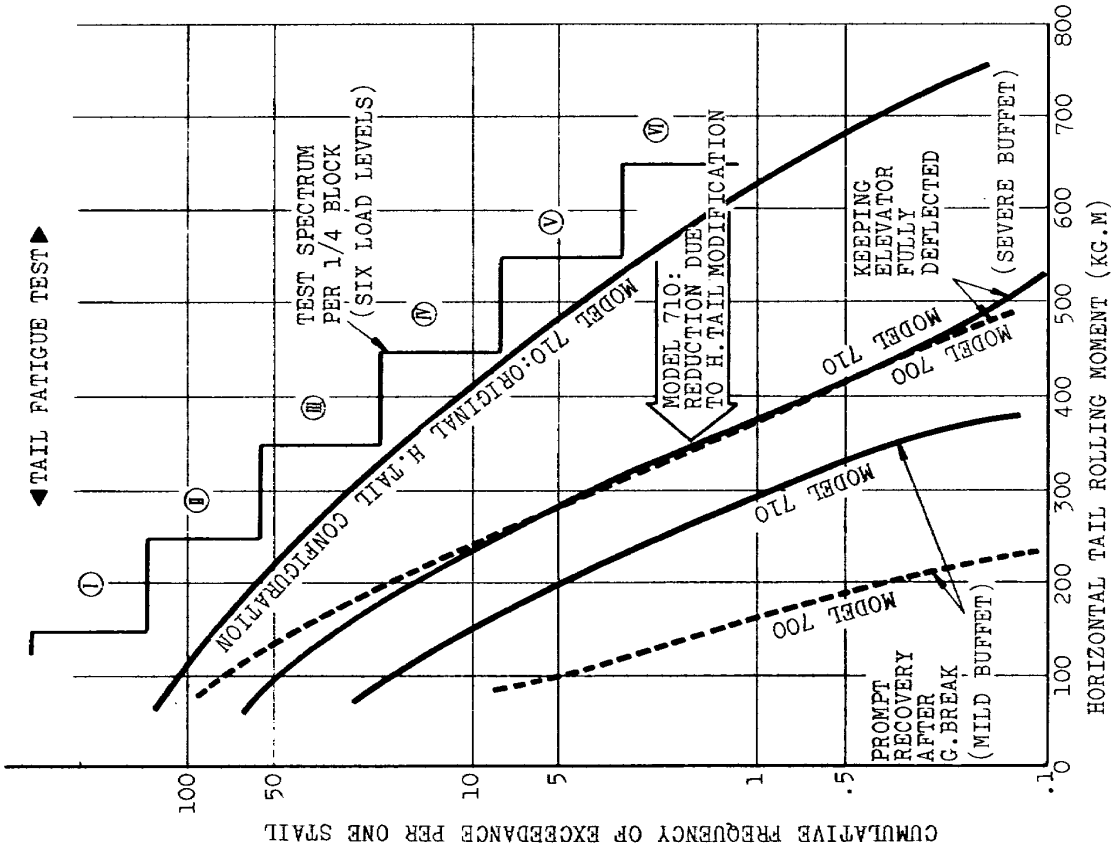

Fig. 26 Tail Buffet Load Spectrum

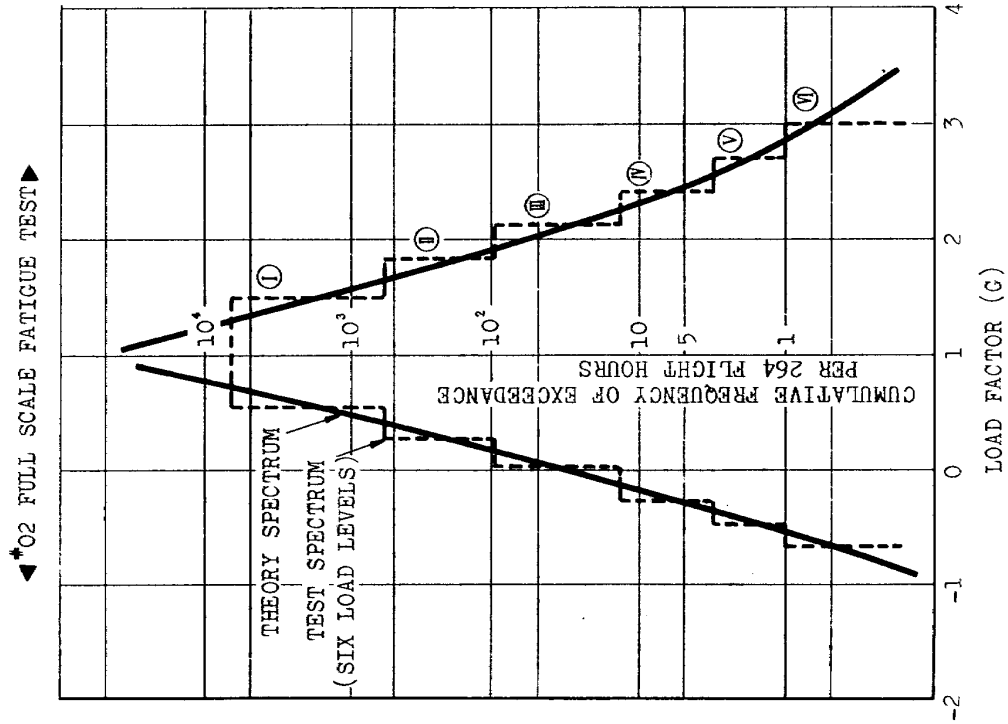

Fig. 25 Flight Load Spectrum

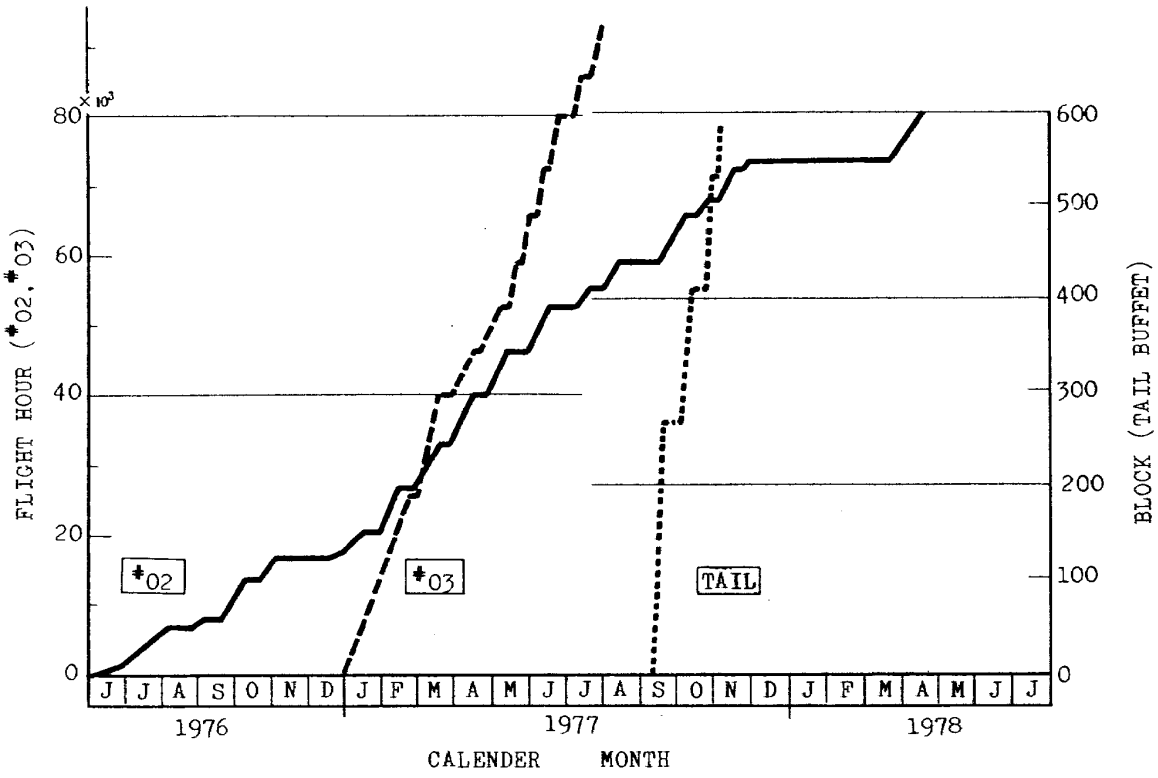

Fig. 27 Fatigue Test Progress

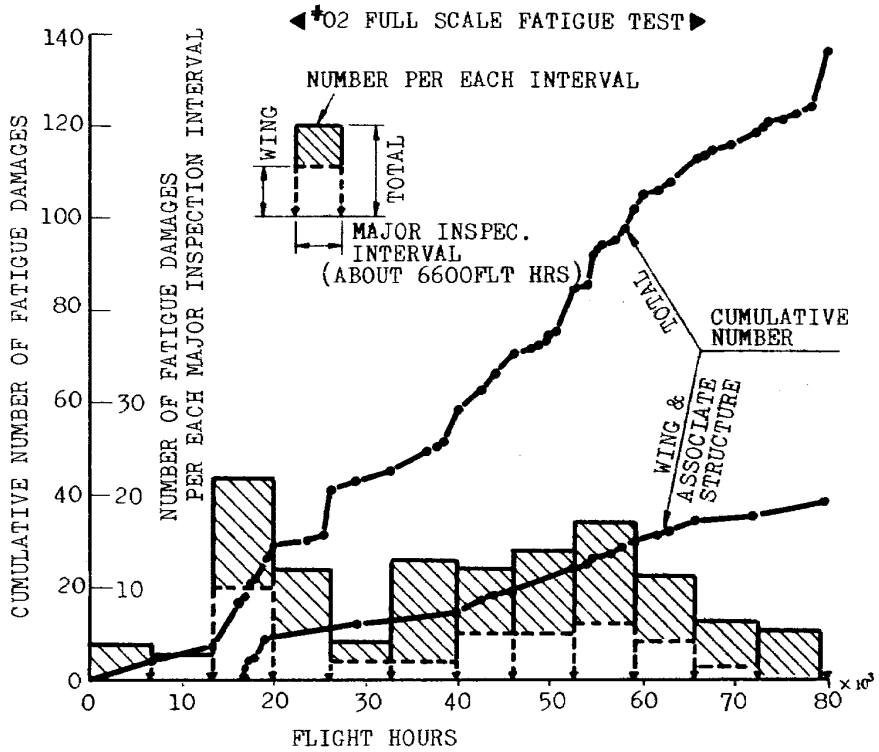

Fig. 28 Occurrence of Fatigue Damages

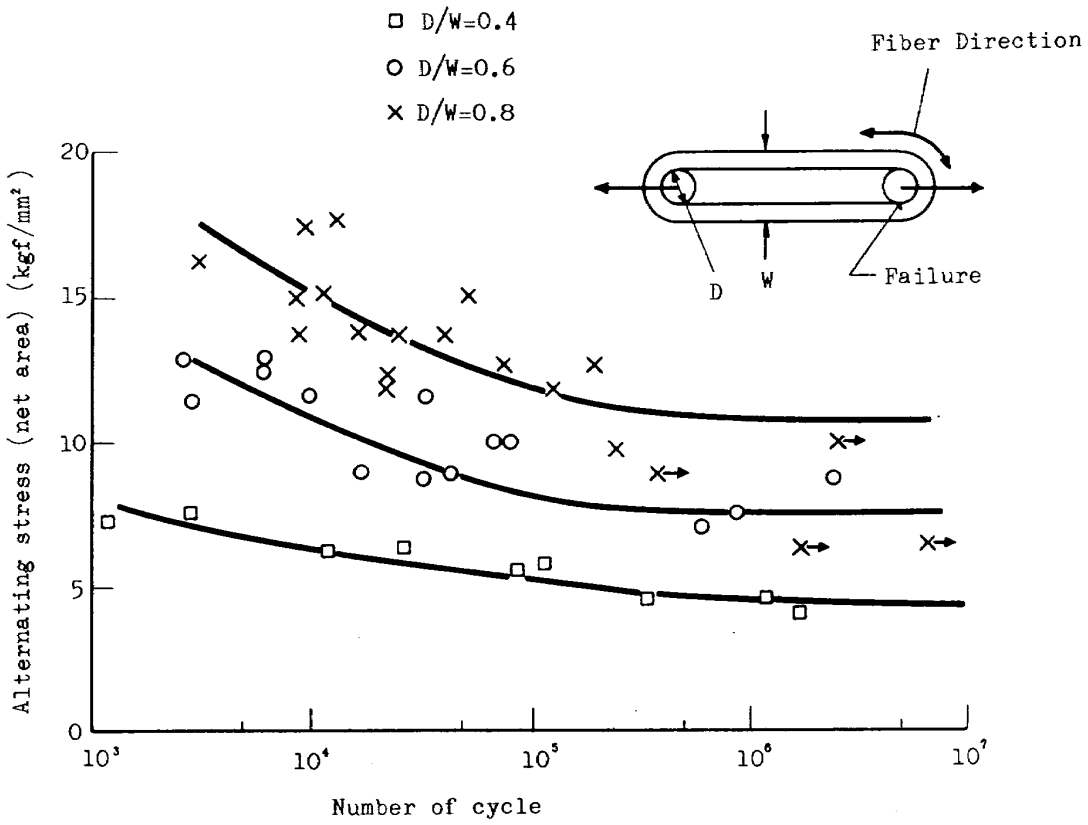

Fig. 29 Test Results of GFRP Lugs

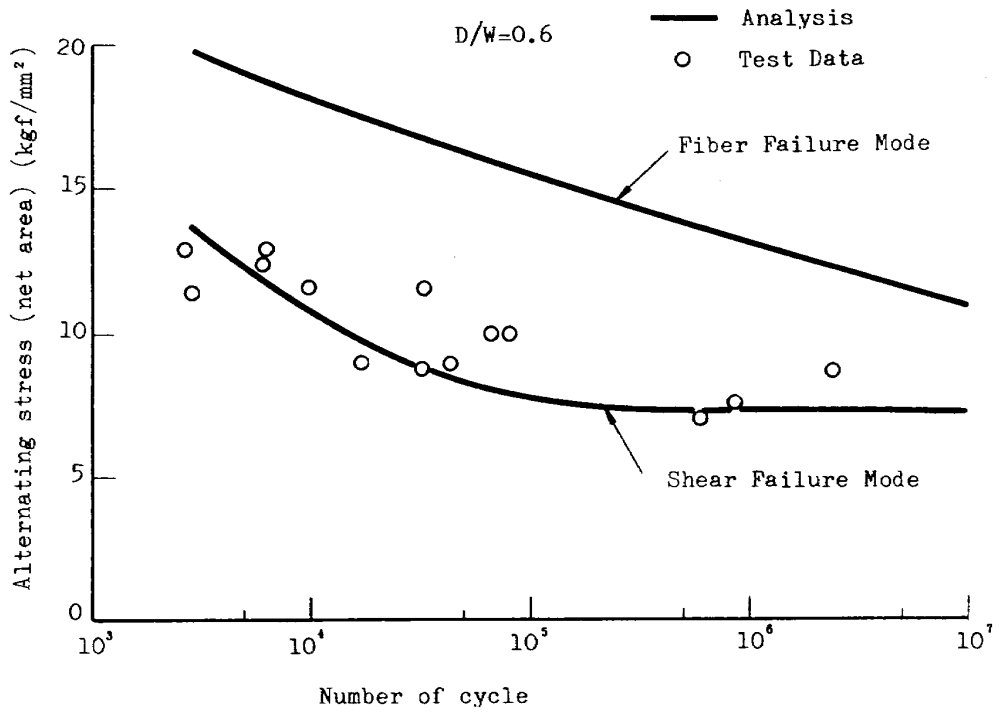

Fig. 30 Correlation between Tests and Analysis

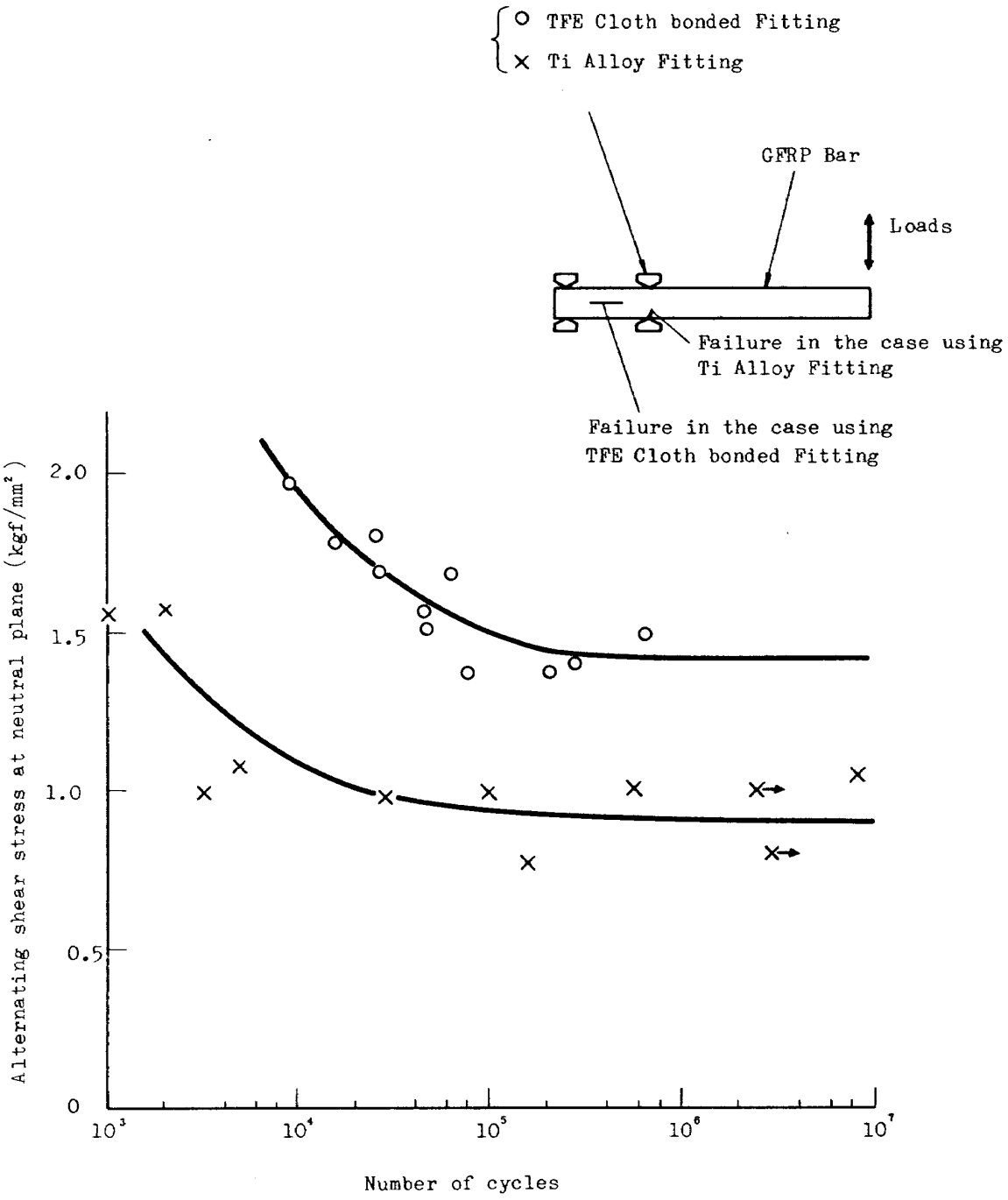

Fig. 31 S-N Curves for Surface Strength of GFRP Bars

TECHNICAL MEMORANDUM OF NATIONAL
AEROSPACE LABORATORY
TM-394T

航空宇宙技術研究所資料394T号(欧文)

昭和54年10月発行

発行所　航空宇宙技術研究所
東京都調布市深大寺町1880
電話武蔵野三鷹(0422)47-5911(大代表)〒182
印刷所　株式会社　共進
東京都杉並区久我山4－1－7(羽田ビル)

Published by
NATIONAL AEROSPACE LABORATORY
1,880 Jindaiji, Chōfu, Tokyo
JAPAN

Printed in Japar